ABSTRACT

Title of Document: **Electrically Induced Gelation, Rupture, and Adhesion of Polymeric Materials**

Ankit Gargava, Doctor of Philosophy, 2017

Directed By: Professor Srinivasa R. Raghavan
Department of Chemical and Biomolecular Engineering

There has been considerable interest in developing stimuli-responsive soft materials for applications in drug delivery, biosensing, and tissue engineering. A variety of stimuli have been studied so far, including temperature, pH, light, and magnetic fields. In this dissertation, we explore the use of electric fields as a stimulus for either creating new soft materials or for rupturing existing ones. Our materials are based typically on biocompatible polymers such as the polysaccharides alginate, chitosan, and agarose. We also discuss the advantages and disadvantages of electric fields over other stimuli.

First, we describe the use of electric fields to form transparent and robust alginate gels around an initial mold made of agarose. Moreover, we can melt away the agarose by heat, leaving us with hollow alginate tubes. In our technique, a tubular agarose mold with dissolved calcium chloride ($CaCl_2$) is placed in a solution of sodium alginate. A voltage of ~ 10 V is then applied, with the mold as the anode and the container as the cathode. As the Ca^{2+} ions migrate from the mold towards the cathode, they contact the alginate chains at the mold surface. In turn, the Ca^{2+} crosslinks the alginate chains into a gel, and the gel grows outward with time. The technique can be used to grow multiple layers of alginate,

each with a different content, and it is also safe for encapsulation of biological species. Complex tubular structures with multiple branches and specific patterns can be created.

Next, we report that electric fields can be used to rupture particles formed by ionic complexation. The particles under study are typically in the microscale (~ 200 μm radius) and are either uniformly crosslinked microbeads (e.g., alginate/Cu^{2+}) or microcapsules formed by complexation of oppositely charged polymers (alginate and chitosan). When these particles are placed in aqueous solution and subjected to an electric field of about 10 V/cm (applied remotely, i.e., electrodes not in contact), the particles rupture within about 5 min. A possible mechanism for the electric-field-induced disruption is discussed. We also use the above particles to create electrically actuatable valves, where the flow of a liquid occurs only when the particle blocking the flow is disrupted by the field.

In our final study, we show that polyelectrolyte gels and beads can be rapidly induced to adhere by an electric field. We typically work with crosslinked acrylate hydrogels made with cationic co-monomers, and anionic beads made by contacting alginate with Ca^{2+}. When the cationic gel (connected to an anode) is contacted for just a few seconds with the anionic bead (connected to a cathode) under a voltage of ~ 10 V, the two form a strong adhesive bond. When the polarity of the electrodes is reversed, the phenomenon is reversed, i.e., the gel and bead can be easily detached. We suggest that the adhesion is due to electrophoretic migration of polyelectrolyte chains, resulting in the formation of polyion complexes. Applications of this reversible adhesion are discussed for the pick-up and drop-off of soft cargo, and for the sorting of beads.

Electrically Induced Gelation, Rupture, and Adhesion of Polymeric Materials

By

Ankit Gargava

Dissertation submitted to the Faculty of the Graduate School of the

University of Maryland, College Park, in partial fulfillment of

the requirements for the degree of

Doctor of Philosophy

2017

Advisory Committee:

Professor Srinivasa R. Raghavan, Department of Chemical & Biomolecular Engineering, Advisor

Professor Kyu Yong Choi, Department of Chemical & Biomolecular Engineering

Professor Chunsheng Wang, Department of Chemical & Biomolecular Engineering

Professor Taylor J. Woehl, Department of Chemical & Biomolecular Engineering

Professor Gregory F. Payne, Fischell Department of Bioengineering, Dean's Representative

Acknowledgements

There have been many people who have walked alongside me during the last five years. They have guided me, placed opportunities in front of me and showed me the doors that might be useful to open. I would like to take this opportunity to thank them.

First, I would like to thank my advisor, Prof. Srinivasa Raghavan, for giving me the opportunity to pursue my interest and be a part of his research group. His continuous guidance, motivation and wisdom is the reason I feel proud of the research work we have done together. He has provided me the freedom to work on the ideas that fascinates me. He has been a great mentor and heavily influenced how I tackle scientific and technical challenges. He has made me the scientist I am today. For that, I am truly grateful.

I would like to thank Prof. Gregory Payne for our useful discussions on electrochemical processes. I would also like to thank Prof. Choi for providing me the opportunity to work with him on polymerization simulation project. It gave me a flavor of computational research. I would like to acknowledge Dr. Yogesh Joshi for inspiring me to pursue a PhD degree and for his support and motivation.

I am grateful to my lab group members. Sincere thanks to Dr. Bani Cipriano and Dr. Joe White for their advice on all things rheology; Dr. Hyuntaek Oh, Dr. Chanda Arya, and Dr. Xuefeng Li for all the technical discussions that helped me in my research. Special thanks to Dr. Jasmin Athas, Dr. Annie Lu, Brady Zarket and Kerry DeMella for teaching me literally everything in the lab (and few things outside), for their constant effort to make

me follow all the lab safety rules and for all the endless research idea discussions we had. I would also like to thank Dr. Charles Kuo, James Liu, Niti Agrawal, Toniya Acharya, Umang Khamar, Chunxue, Hanchu and all the group members for the good times in the lab. It has been fun doing research with you all. I would like to acknowledge undergraduate students Rahul Ragunathan, Rui Ponte, Javier Vandeyar, Prateeti Sarker, Hema Manivannan and Sina Atai, and high school student Kaitlyn Hennacy for their help in conducting some of the experiments.

To my friends, Agraj, Prakhar, Sandesh, Sandeep, and Varun. Acknowledgment would not be enough to express my gratitude; your constant support and motivation has been tremendous, especially during the tough times. Thanks for always being there when I needed the most. I'm so grateful to have you all in my life.

Finally, and most importantly, I would like to acknowledge the support, and sacrifice from my family without whom this would not have been possible. My brother, Anuj, for being with our parents when I couldn't. My mom, who always puts us before her needs. I am truly indebted for her unconditional love and care. My dad, my role model, has been my biggest inspiration to uphold highest of values in every aspect of life. Thank you.

Table of Contents

List of Figures

Chapter 1

Introduction and Overview

1.1 Problem Description and Motivation

Processes in nature frequently occur as a response to some external trigger. For instance, leaves in plants open and close their stomatal pores based on humidity and sunlight; ectothermic animals regulate their metabolic rate depending on external temperature; and blood clotting mechanism in our body is initiated in response to the damaged blood vessel. All these processes involve "sensing" a stimulus, which is then transduced to a "response". Inspired by nature, researchers are trying to develop stimuli-responsive materials that exhibit changes based on their surrounding environment or external fields. In the field of soft matter, responsive materials based on polymers[1,2] have been extensively investigated. The typical stimuli to which these materials are exposed to include temperature, pH, solvent quality, and the presence of solutes such as salts.

In recent years, our lab has been engaged in efforts to explore new kinds of stimuli for modulating soft materials. For example, we have investigated light[3] and biomolecules[4] to trigger changes in polymeric and colloidal materials. Each of these stimuli has its shortcomings. For example, pH and temperature, can be applied over a large volume, but they are difficult to apply at a precise point in a given volume. In comparison, light can be controlled and directed at a precise point, but it gets rapidly attenuated as it passes through water or through aqueous gels. Thus, the response-time in the case of light is much higher

than with some of the other stimuli. On the whole, there is a need for a stimulus that is easy to apply, control, direct, and generate a rapid response.

Electricity as a stimulus seems a particularly interesting option. Electric fields can be easily turned on and off, can be spatially controlled, usually give faster response, and can be integrated to work at a remote location. Despite these advantages, the use of electric fields to modulate soft materials has its own challenges, the chief among which is that most organic materials such as polymers as well as aqueous gels are not electrically conductive (some may conduct ions, but not electrons). Thus, electrical response has usually required rather exotic materials like conducting polymers, or conducting particles like carbon nanotubes. At the moment, there are a few examples of electrically responsive soft materials, which are used in actuators,[5,6] drug delivery,[7] and tissue engineering.[8,9] While there is a long history of electrically responsive systems,[10] for this field to truly advance, it will require new effects to be demonstrated with simple and biocompatible materials that are readily available. This is the focus of the present study.

1.2 Proposed Approach

In this dissertation, we describe three new electro-responsive systems in which we have found new phenomena that have not been described so far in the literature. These are described below.

1.2.1 Electrically Induced Gelation

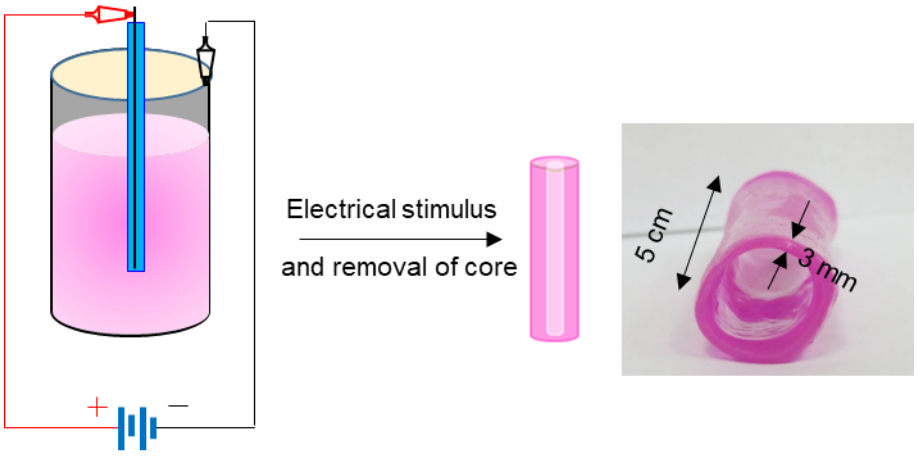

Figure 1.1. Electrically induced formation of an alginate gel around an agarose mold filled with divalent cations. Hollow three-dimensional structures can be developed using the technique (Chapter 3).

In our first study (Chapter 3), we show that electric fields can induce the formation of biopolymer gels around an initial mold. We start with a thermoresponsive polymer (agarose) mold that contains dissolved calcium chloride ($CaCl_2$) and thereby acts as the source of cations. This mold, shown as a cylinder in Figure 1.1, is placed in an alginate solution and a bias is applied, with the mold as the anode and the container wall as the cathode. As the Ca^{2+} ions migrate from the mold towards the cathode, they contact the alginate chains at the surface of the mold. In turn, the cations crosslink the alginate chains into a gel, and a layer of the gel grows around the mold. The gel thickness increases with time over which the electric field is applied. When the field is switched off, the gel stops growing. Once a gel of desired thickness has formed, we can melt away the agarose by heat, leaving us with a hollow alginate tube, as shown in Figure 1.1. The technique can be used to grow multiple layers of alginate, each with different payloads of interest. It is also

safe for encapsulation of biological species, such as bacteria. Complex tubular structures with multiple branches and specific patterns can also be created.

1.2.2 Electrically Induced Particle Rupture

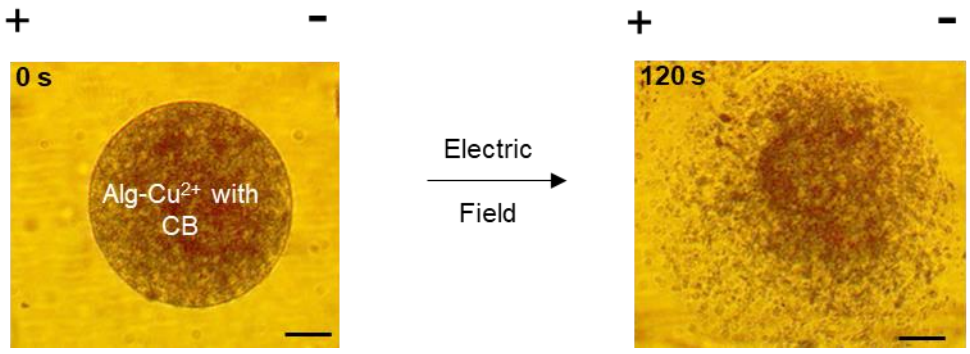

Figure 1.2. Electrically induced rupturing of particles formed by ionic complexation (such as alginate/Cu^{2+} microbeads) (Chapter 4). Scale bars: 100 μm.

In Chapter 4, we report that electric fields can be used to rupture particles formed by ionic complexation. The particles studied are typically in the microscale and are synthesized using a microfluidic setup by adding solutions of alginate (an anionic biopolymer) dropwise into a solution of a divalent cation (e.g., Cu^{2+}). These particles are placed in an aqueous solution containing a low concentration of salt and subjected to a remote electric field (i.e., the electrodes are placed far from the particles). As shown in Figure 1.2, the particles rupture within a few minutes. Such rupture is not observed if the particles are crosslinked by covalent rather than ionic bonds. A possible mechanism for the phenomenon is discussed. We also use the above particles to create electrically actuatable valves, where the flow of a liquid occurs only when the particle blocking the flow is disrupted by the field.

1.2.3 Electrically Induced Adhesion of Beads to Gels

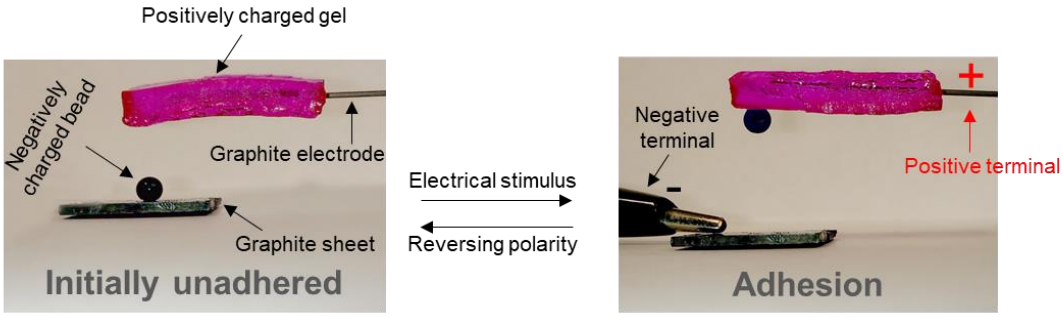

Figure 1.3. Adhesion of an anionic bead to a cationic gel when the two are contacted under an electric field with specific directional bias (Chapter 5).

Finally, in Chapter 5, we show that polyelectrolyte gels and beads can be rapidly induced to adhere by an electric field. When a cationic gel (connected to an anode) is contacted for just a few seconds with an anionic bead (connected to a cathode) under a voltage, the two form a strong adhesive bond (Figure 1.3). This adhesion is reversible: when the polarity of the electrodes is reversed, the gel and bead can be easily detached. The above effects are seen for both physically and chemically crosslinked gels and beads, as well as for gel-gel and bead-bead pairs. The adhesion is probably due to electrophoretic migration of polyelectrolyte chains, resulting in the formation of polyion complexes. Applications of this reversible adhesion are discussed for the pick-up and drop-off of soft cargo, and for the sorting of the beads.

1.3 Significance of This Work

We believe the significance of this work is two-fold. First, there are direct applications of the abilities demonstrated in this study, i.e., the electrically induced gelation, disruption and adhesion of soft materials. Second, our study substantially

advances the use of electric fields as a stimulus in soft materials research. Specific applications are worth mentioning. In the context of tissue engineering using hydrogels, cell growth, differentiation, and morphology depend heavily on the hydrogel geometry and stiffness.[11,12] The technique described in Chapter 3 allows us to develop gels of alginate (a well-known biopolymer) in specific geometries (such as branched tubes) and with desired stiffness. In Chapter 4, we demonstrate rupturing of biopolymer capsules and beads using electric field, and we also showed how such effects could be used to construct valves. These results could pave the way for devices where encapsulated drug can be released into the environment by activating an electrical trigger.[13] Finally, the reversible adhesion illustrated in Chapter 5 could potentially be utilized for biological sealant applications or in new types of adhesive patches. Overall, we anticipate that our work will generate considerable interest in the use of electric fields as a viable stimulus to modulate soft matter.

Chapter 2

Background

This dissertation focuses on electro-responsive biopolymer materials whose interactions with electric fields can give rise to interesting behavior. In this chapter, we provide a brief introduction to the main biopolymers used in this work (alginate, chitosan, and agarose). We will also discuss the relevant effects expected when soft materials are exposed to electric fields.

2.1 Biopolymers

Alginate. Sodium alginate is an anionic polysaccharide obtained from brown seaweed. It is widely used for biomedical applications[14] due to its low cost, biocompatibility, low toxicity, and its ease of crosslinking. It is a linear unbranched polymer consisting of blocks of 1,4-linked β-D mannuronic acid (M) and α-L guluronic (G) residues (Figure 2.1a).[15] The G-blocks of alginate can interact with specific multivalent ions such as Ca^{2+}, Sr^{2+}, Cu^{2+}, or Fe^{3+}. These cations form "egg-box" junctions, which results in the conversion of an alginate solution into a crosslinked alginate gel (Figure 2.1b). The strength of these alginate gels depends on the ratio of M/G content, the molecular weight and concentration of alginate, and the type of multivalent cation.[16] Alginate gels are known to slowly disintegrate in NaCl solution due to ion exchange between the Na^{+} ions and the multivalent cations in the gel.[17] The kinetics of this exchange depends on the affinity of the multivalent

cations towards alginate.[18] Cu^{2+} forms a relatively stable gel of alginate, which does not easily disintegrate in NaCl solution,[17] and is therefore used in Chapter 4.

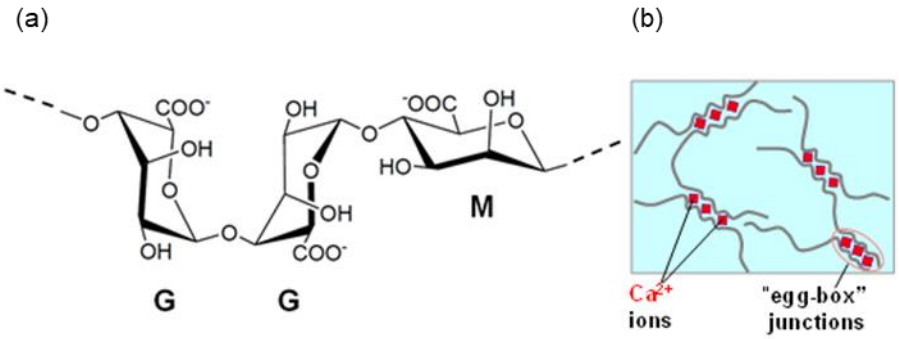

Figure 2.1. (a) Structure of alginate with β-D-mannuronate (M) and α-L-guluronate (G) residues (adapted from Pawar[15]). (b) Schematic demonstrating gelation of alginate upon addition of calcium ions. The zones where crosslinking occurs are called "egg-box" junctions.

Chitosan. Chitosan is a cationic polysaccharide derived from the deacetylation of chitin that is present in the hard shells of insects and crustaceans.[19] While chitin is insoluble in water, its deacetylated form, i.e., chitosan is water-soluble. Chitosan is composed of random β-(1,4) linked D-glucosamine and N-acetyl-D-glucosamine sugars (Figure 2.2a). The free amines generated by deacetylation become ionized in acidic media, making chitosan water soluble.[20] The cationic nature of chitosan also gives it antimicrobial properties. Chitosan is used in a variety of biomedical applications ranging from tissue engineering and wound dressings to drug delivery.[19-21] Chitosan can be crosslinked into a gel either by chemical crosslinkers (like dialdehydes[22]) or physical crosslinkers (like negatively charged surfactants[23] or multivalent anions[24]). Figure 2.2b shows the chemical crosslinking of chitosan by glutaraldehyde and Figure 2.2c shows the physical crosslinking of chitosan by anionic surfactants such as sodium dodecylbenzenesulfonate (SDBS). Due

to the latter type of interaction, capsules can be formed by introducing an aqueous droplet containing chitosan into a solution of SDBS.

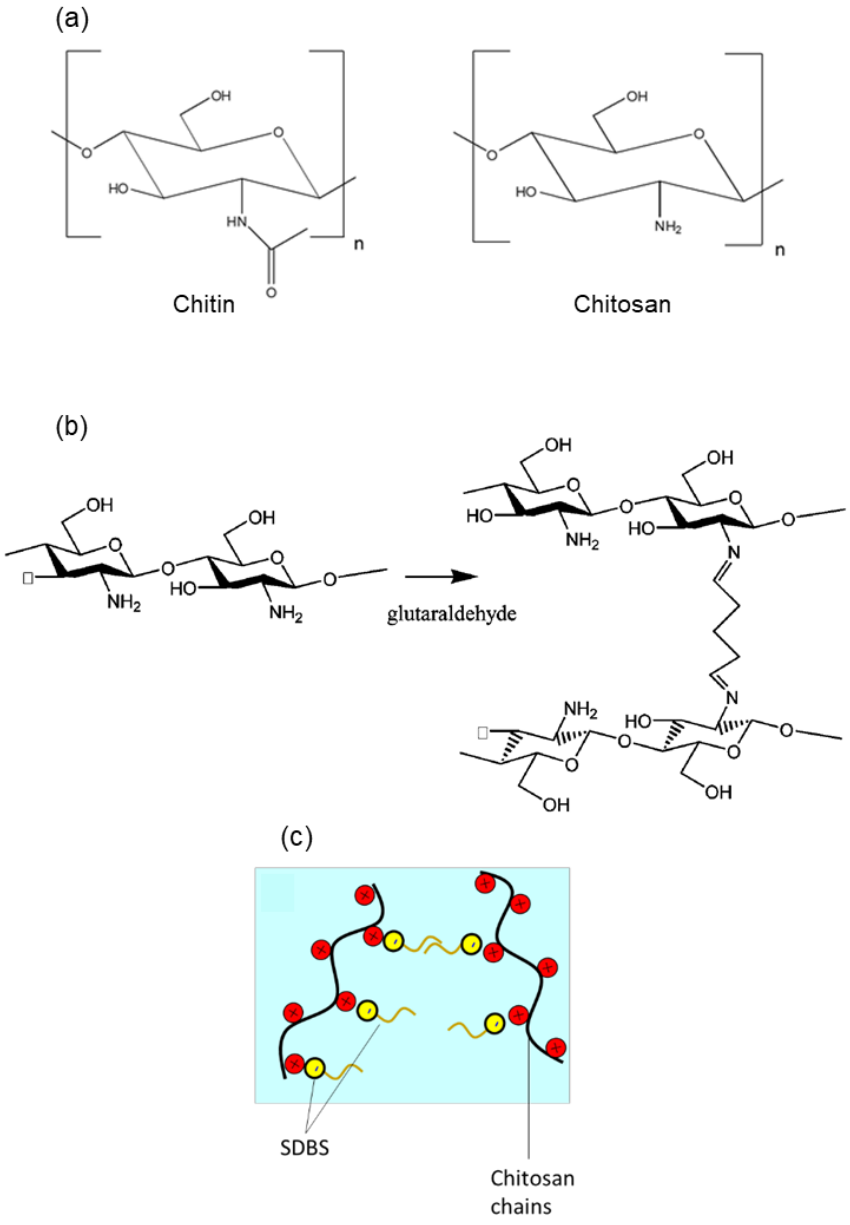

Figure 2.2. (a) Structures of the monomer sugars in chitin and chitosan. The N-acetyl-D-glucosamine sugar in chitin is deacetylated to generate the D-glucosamine sugar in chitosan. (b) Chemical crosslinking of chitosan chains by glutaraldehyde (adapted from Macquarrie[22]). (c) Physical crosslinking of the amines on chitosan by anionic surfactants like SDBS.

Agarose. Agarose is a neutral polysaccharide extracted from seaweed. It consists of alternating 1,3 linked β-D-galactose and 1,4 linked 3,6-anhydro-α-L-galactose residues (Figure 2.3a).[25] It is one of the two main components of agar, the other being agaropectin. Agarose is insoluble in water at room temperature. It dissolves in near-boiling (80–90°C) water and forms a gel upon cooling to 30–45°C. The gelation mechanism involves a shift from random coils in the sol state to a double helix in the initial gel state, and then to bundles of double helices in the final gel state (Figure 2.3b), which are connected into a network.[26] Agarose forms strong gels at very low concentrations. The strength of the gel can be adjusted by changing agarose concentration. Agarose gels melt upon heating, i.e., the gels are thermoreversible. Agarose gels are used in a variety of applications including electrophoresis,[27] cell culture,[28] and therapeutics.[29]

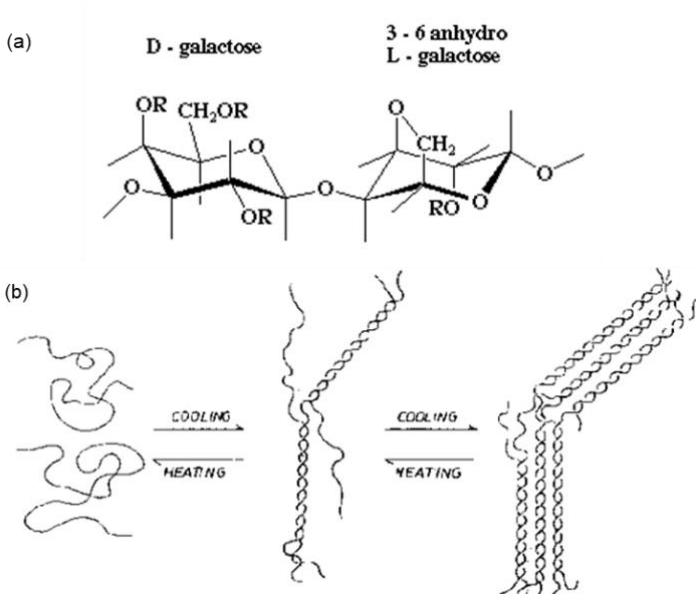

Figure 2.3. (a) Structures of the monomers in agarose. (b) Agarose gelation mechanism (adapted from Armisen[30]).

2.2 Electric-Field Induced Effects

2.2.1 Ions in Electrolyte Solutions

Ions in a salt (electrolyte) solution move randomly in all directions. When a voltage (and thereby an electric field) is applied across the solution, the ions experience electrical forces. Cations move towards the cathode (negative electrode) and anions move towards the anode (positive electrode), and this motion is called electrophoresis. The ions soon attain a constant drift velocity due to the balance between electrical and drag forces. The ions may or may not participate in electrochemical reactions at the electrodes. Non-reacting cations accumulate near the cathode and the corresponding anions near the anode. In addition, electrolytic reactions occur at the electrodes, provided the voltage exceeds the standard electrochemical potential of water (1.23 V). As shown below, H^+ ions are produced at the anode and OH^- ions are produced at the cathode. This, in turn, leads to pH gradients in the solution.[31]

$$2H_2O\,(aq) \rightarrow O_2(g) + 4H^+(aq) + 4e^- \qquad (at\ anode)$$

$$2H_2O\,(aq) + 2e^- \rightarrow H_2(g) + 2OH^-(aq) \qquad (at\ cathode)$$

2.2.2 Polyelectrolytes in Solution

Polyelectrolytes, i.e., charged polymer chains, dissolved in solution act similar to smaller ions under an electric field. That is, they electrophoretically migrate towards the oppositely charged electrode. However, due to their larger size, polyelectrolytes take much longer to migrate. Moreover, the polyelectrolytes can undergo a phase change to form gels or precipitates near or at the electrodes. This is due to neutralization of the charged groups

on the backbone of the polyelectrolyte chains, which in turn occurs due to the pH gradient near the electrode.[32,33] When the gel/precipitate is formed at the electrode, it results in the deposition of a film, and the process is called electrodeposition. Figure 2.4a shows that chitosan (a cationic polyelectrolyte) is deposited at the cathode due to the higher pH there (deposition occurs when the pH exceeds the pKa of chitosan).[32] Similarly, Figure 2.4b shows that alginate (an anionic polyelectrolyte) can be deposited at the anode due to the low pH there.[32,33]

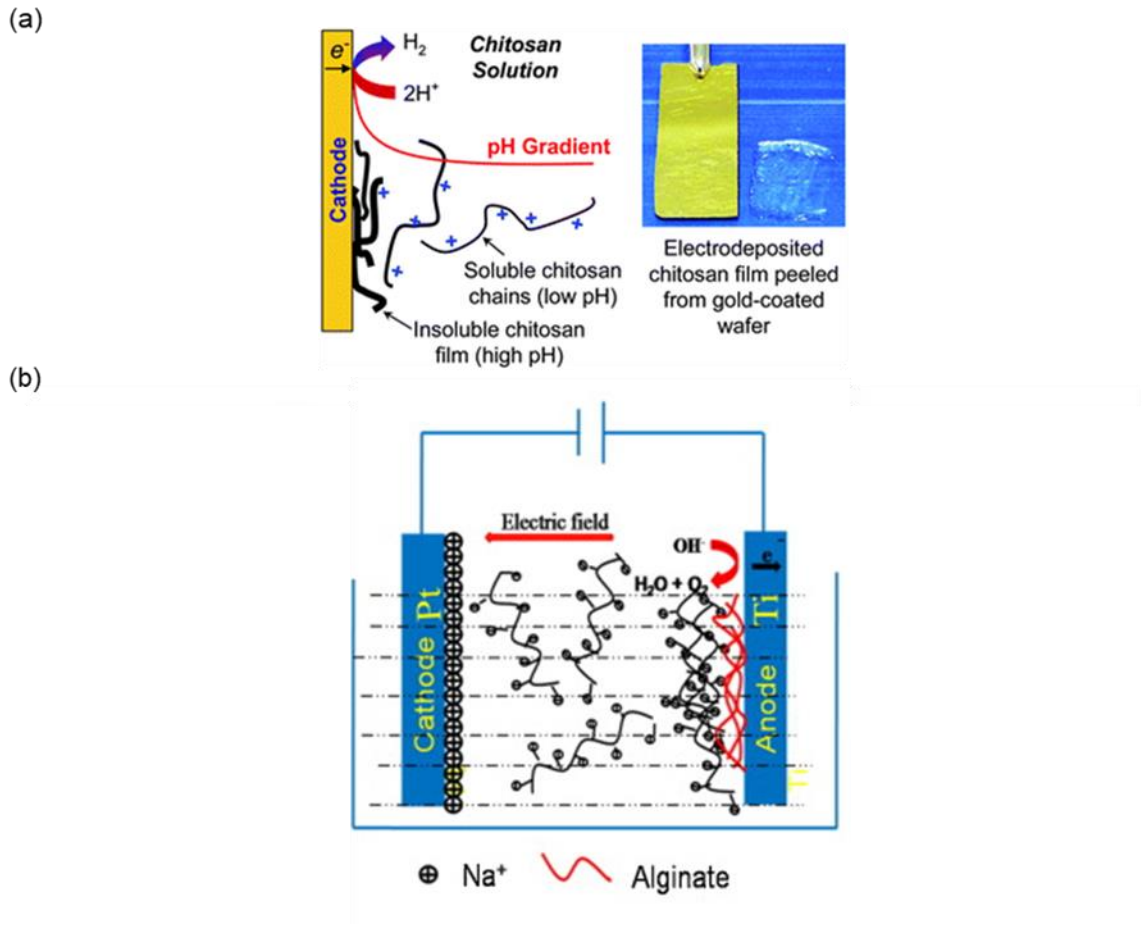

Figure 2.4. (a) Electrodeposition of chitosan at cathode (adapted from Liu[32]) (b) Electrodeposition of alginate at anode (adapted from Wang[33])

2.2.3 Polyelectrolyte Gels

Polyelectrolyte gels are three-dimensional networks of charged polymer chains that have the consistency of a solid but allow the transport of small molecules within the network. The chains may be connected by physical or chemical bonds. Figure 2.5 shows the schematic of an anionic polyelectrolyte hydrogel.

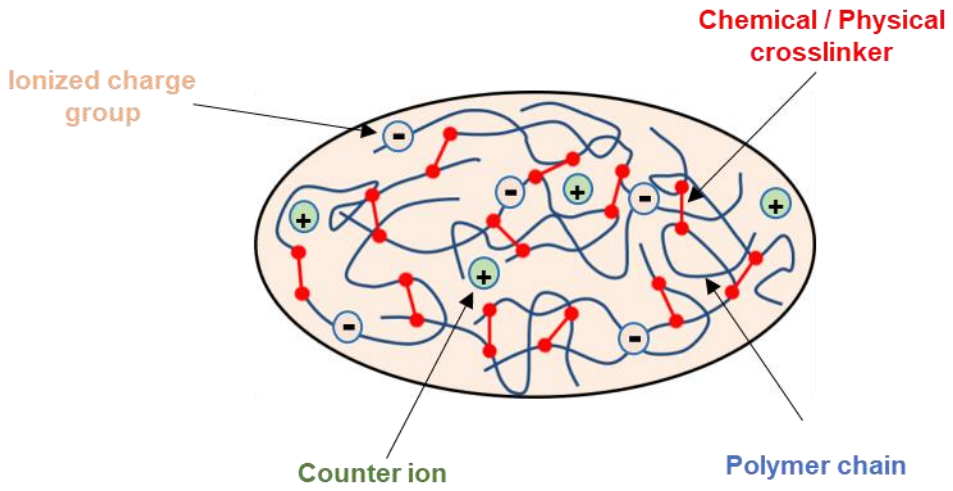

Figure 2.5. Components of an anionic polyelectrolyte hydrogel. Charged polymer chains are physically or chemically crosslinked into a three-dimensional network that is swollen in water (inspired from Morales[34]).

Due to the ionizable groups along the backbones of the polyelectrolyte chains as well as the mobile counterions in the network, polyelectrolyte gels can show a response under an electric field. Figure 2.6 shows different effects that can be induced in such gels by a field.[34] Each effect is briefly described below.

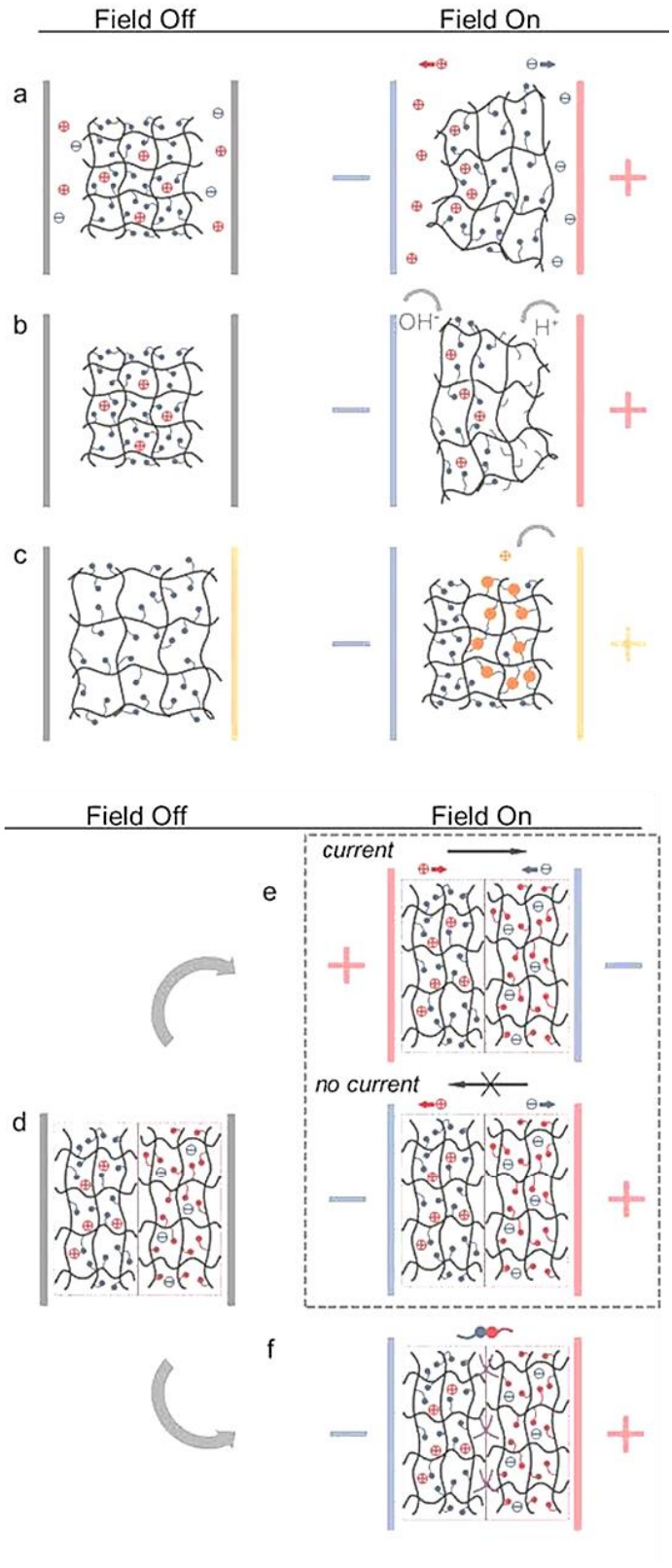

Figure 2.6. Different effects induced in polyelectrolyte gels under an electric field (adapted from Morales[34]).

Anisotropic Swelling Due to Osmotic Pressure Differences (Figure 2.6a). When an anionic gel is in an electrolyte, the electric field causes redistribution of ions both inside and outside the gel. The redistribution of ions is a result of permselectivity, i.e. preferential migration of cations through anionic gels (and vice versa for cationic gels). As a result, the osmotic pressure difference between the gel and the solution on the anode side is much larger than that on the cathode side. This causes the anionic gel to swell on the anode side and shrink on the cathode side.

Anisotropic Swelling Due to Electrolysis of Water (Figure 2.6b). As discussed in the previous section, electrolysis results in pH gradients from the electrodes. When an anionic gel is placed in an electrolyte, the high pH regions on the cathode side causes more ionization of the fixed charge groups on the polyelectrolyte backbone, thereby causing swelling on the cathode side. The acidic region on the anode side causes de-ionization of fixed charges and leads to shrinking on that side.

Ionic Crosslinking Due to Oxidation of Anodic Material (Figure 2.6c). When an anionic gel is placed in an electrolyte, and the electrode material can participate in an electrochemical reaction, the gel can be modified. For example, consider the case when the gel is based on alginate and the anode is made of copper. Under the electric field, copper gets oxidized to Cu^{2+} ions, which can crosslink alginate chains and therefore increase the crosslink density on the anode side. The anode side of the gel would therefore become stiffer and swell less.

Ionic Conductivity Due to Polyelectrolyte Interfaces (Figure 2.6d, e). When an anionic gel is kept in contact with a cationic gel, the system can behave as an organic diode (rectifier). That is, connecting the anode to the anionic gel and the cathode to the cationic gel would allow counterions to migrate to their respective electrodes, i.e. counterions of the anionic gel would cross the interface and move towards the cathode and counterions of the cationic gel would cross the interface and move towards the anode. The counterions thus allow a current to flow. If the polarity is reversed, the counterions cannot cross the interface and there is no current. Thus, the sandwich of an anionic and a cationic gel can act as a current rectifier.

Adhesion Between Polyelectrolyte Interfaces (Figure 2.6d, f). When a cationic gel connected to the anode and an anionic gel connected to the cathode are brought together, a strong adhesion can arise between the interfaces. The migration of anionic chains towards the anode and cationic chains towards the cathode causes their interpenetration and formation of polyion complexes. This leads to adhesion. The gels can be detached upon reversing the polarity.

Chapter 3

Electro-Formation of Alginate Gels

3.1 Introduction

In this chapter, we will describe a new technique to form alginate gels upon applying an electric field. Our technique is rapid, biocompatible and can be used to form gels in desired geometries. As we will show, the mechanism for gelation relies on electrophoretic migration of charged species instead of electrolysis of water. The geometrical flexibility of our technique arises due to the fact that instead of using a rigid electrode as the surface for the alginate gel to form, we use a gel of another biopolymer called agarose. Agarose is a thermo-responsive polysachharide, extracted from seaweed, which shows a sol-gel transition based on temperature. We start by mixing $CaCl_2$ with agarose and making a template in the desired geometry. When we put this template in an alginate solution and apply electrical bias with a specific polarity, an alginate gel is formed around the agarose template within minutes. This gelation is a result of migration of Ca^{2+} ions and alginate chains towards their respective electrode under electrical force and undergoing gelation through "egg-box" junctions upon contact. The shape of the alginate gel is an inverse replica of the original mold. The resultant alginate gel is transparent, robust, and the process is mild and compatible with biological species. Gels in several 3-D architectures including multilayer tubes and patterned structures can be formed by our technique, and many of these cannot be achieved through conventional methods. The simplicity and versatility of the technique should make it attractive to researchers.

3.2 Experimental Section

Materials and Chemicals. Alginate (medium molecular weight, viscosity >= 2000 cP, 2%), calcium chloride dihydrate, and agarose (Type 1-A, low EEO, melting temperature ~88°C, gel point ~35°C) were obtained from Sigma-Aldrich. Graphite pencil electrode (pentel super hipolymer lead, 9mm) was purchased from Staples and super hydrophobic Rust-oleum "NeverWet" spray coating was purchased from The Home Depot. Methylene blue dye was purchased from Sigma-Aldrich and acid red 52 dye was obtained from TCI America. Red (diameter ~ 500 nm) and green (diameter ~ 100 nm) fluorescent latex nanospheres were purchased from Polysciences Inc. All chemicals were used as received.

Agarose Gel Preparation. Agarose gels were prepared by first dissolving weighed amounts of $CaCl_2$ into DI water and heating the solution to above 80°C. Subsequently, 2.5 wt% of agarose was added to the solution and mixture was continuously heated until the agarose was completely dissolved. The hot solution was then poured into test-tubes (1.2 cm diameter, 7.5 cm) containing graphite pencil lead electrode and allowed to cool to room temperature.

Experimental Set-up. Figure 3.1a shows the schematics of the experimental setup used to synthesize alginate gels. The setup was comprised of a DC power source (Agilent E3612A), a graphite pencil lead electrode, and a beaker (diameter 5 cm) wrapped inside with aluminium foil. Cylindrical agarose gel (1 cm diameter, 5.5 cm long) containing graphite pencil lead electrode along its axis was placed along the centre of the beaker with aluminium foil, and filled with 90 gm of 1 wt% alginate. The positive terminal of the power

supply was connected to the graphite pencil lead electrode and the negative terminal was connected to the aluminium foil.

Kinetic study. For kinetic study, disk shaped agarose gel (5.5 mm diameter, 4 mm thick) with graphite pencil lead electrode at its centre was placed in a petridish (diameter 50 mm) filled with 10 gm of 1 wt% alginate. The setup was placed under an inverted microscope (Zeiss Axiovert 135 TV) for optical monitoring. A bias of 10V was applied and bright field images were taken at regular intervals. The images were analysed using ImageJ software.

Rheological Measurements. Cylindrical alginate gels with agarose core were developed by the technique mentioned above. The alginate gels were cut and peeled off from the agarose mold to get rectangular sheets for running the rheological tests. Rheological studies were performed on a Rheometrics AR2000 stress controlled rheometer (TA instruments). All experiments were conducted using 20 mm flat plate geometry at 20°C. Dynamic stress sweep experiments were performed at a frequency of 10 rad/s. Dynamic frequency sweep experiment was then performed in the linear viscoelastic (LVE) region.

Fluorescent Microscopy. Green fluorescent images (NPs and E-coli) were taken using a band pass excitation filter (450-490 nm) and a band pass emission filter (515 - 565 nm). Red fluorescent images were taken using a band pass excitation filter (530-585 nm) and a long pass emission filter (615 nm). The images were overlaid using ImageJ software to visualize both colours simultaneously.

Multilayer Structure Design. Three different alginate solutions were prepared (all with 1% alginate by weight). Solution-1 had alginate mixed with green fluorescent NPs. Solution-2 had just the alginate without any NPs, and solution-3 had alginate mixed with red fluorescent NPs. 0.1 wt% $CaCl_2$ containing agarose disk (6 mm diameter, 6 mm long) was first put in solution-1, followed by solution-2 and then in solution-3. Each step was carried out for 1 min at 10V. The gel was washed with DI water in between each step. The images were taken under fluorescent microscope and superimposed using ImageJ software.

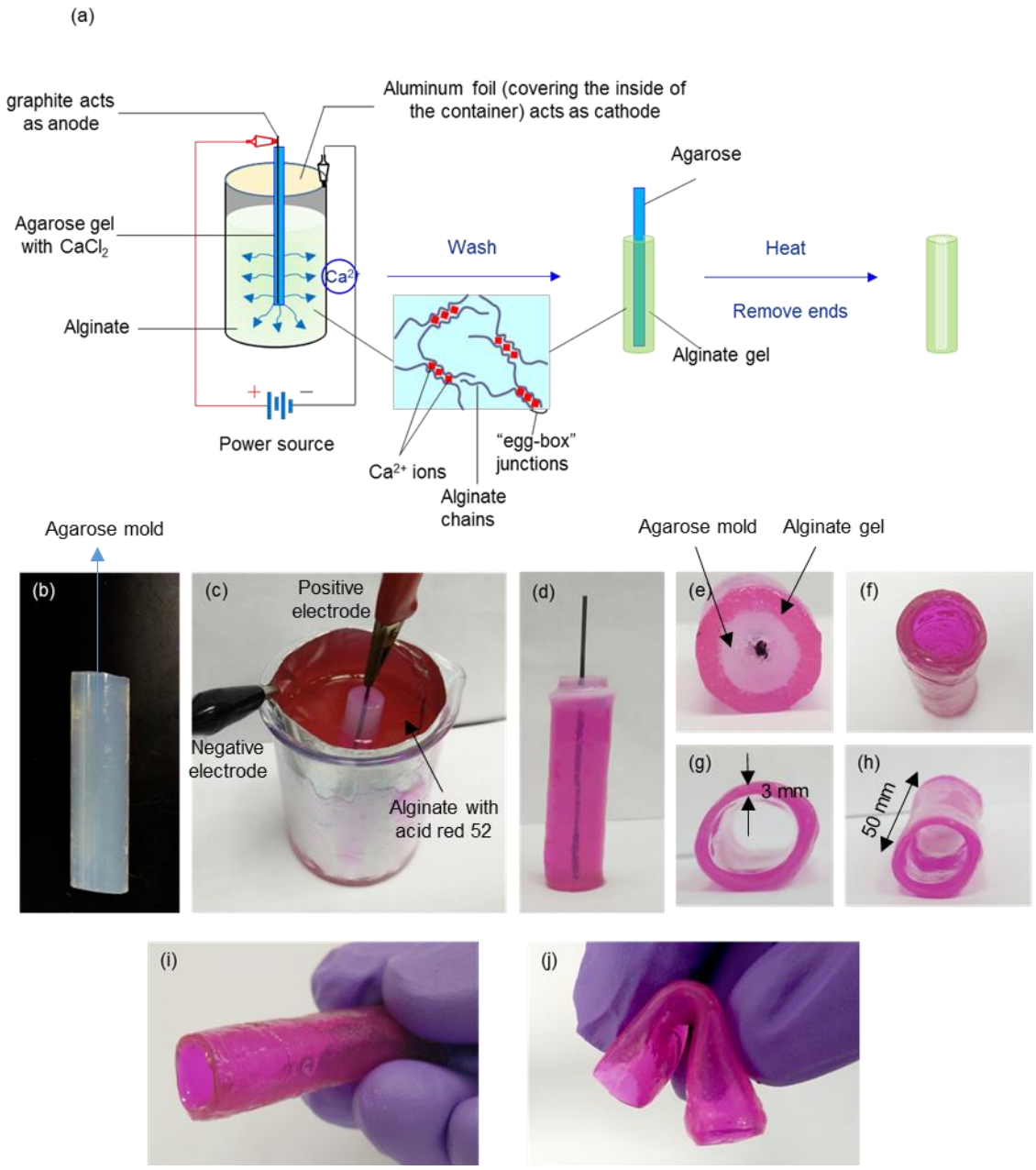

Figure 3.1. Schematics of alginate electro-gelation. (a) The agarose mold contains Ca^{2+} and has a graphite electrode in it, which acts as the anode. The aluminum foil on the inside of the beaker acts as the cathode. When electrical bias is applied, Ca^{2+} ions migrate out of the mold, and crosslink alginate chains into a gel at the mold surface. The alginate gel is formed around the agarose mold. After cutting the ends, the agarose-alginate assembly can be heated to melt away the agarose and obtain a hollow alginate gel. (b, c) Agarose mold and the set-up (the alginate solution is dyed pink-red). (d, e) Alginate gel grown around the mold. (f, g, h) Hollow alginate gel after removing the agarose mold, and this is shown to be strong, yet flexible (i, j).

3.3 Results and Discussion

3.3.1 Electro-Gelation Setup and Formation of Alginate Gel Tubes

Agarose is a thermo-responsive polymer that is insoluble in water at room temperature, but dissolves readily at elevated temperatures. Once dissolved, it remains in a sol state at high temperatures and turns into a gel upon cooling. The sol to gel transition is reversible, i.e., the gel can be liquefied upon heating. We first made a cylindrical agarose gel containing calcium salt. For this, 2.5 wt% of agarose and 0.1 wt% of $CaCl_2$ were added to DI water and dissolved by heating to 80°C. The hot solution was poured into a glass test-tube around a graphite electrode (pencil lead) and allowed to cool to room temperature, whereupon the agarose sets into a gel. Figure 3.1b shows one such agarose gel mold after removing from the test tube (5.5 cm long, 1 cm diameter). The graphite is connected to a DC power supply and it serves as the anode (positive electrode). This mold is placed in a beaker that is wrapped on its inside with aluminum (Al) foil, which serves as the cathode (negative electrode). Sodium alginate at a concentration of 1 wt% is poured in the beaker and it is dyed pink-red (using 0.5 mM of acid red 52 dye) for visualization. A photo of the setup is shown in Figure 3.1c.

We then apply a voltage (typically ~ 10 V), whereupon the Ca^{2+} ions in the agarose mold begin migrating towards the cathode (i.e., away from the mold and into the solution). Correspondingly, alginate chains in the solution migrate towards the anode (i.e., towards the agarose mold). This electrophoresis causes the Ca^{2+} to contact the alginate at the surface of the mold, resulting in an alginate gel layer. Figure 3.1a shows a schematic of the entire process. Note that the divalent Ca^{2+} cations bind to the anionic alginate chains along zones

between adjacent chains, referred to as “egg-box” junctions. The net result is that the alginate chains are crosslinked into a gel network. The thickness of the gel layer around the mold grows over time, but when the voltage is switched off, no further growth occurs. Figure 3.1d and 3.1e show a pink-red alginate gel around the agarose mold, which is formed in 5 min of applying the voltage. From the cross-section view (Figure 3.1e), we infer that the gel is 3 mm thick at this point. Next, we place the agarose-alginate assembly in a hot water bath at 80°C, which causes the central agarose mold to be dissolved away, leaving behind a hollow tubular gel of alginate (with the tube wall being 3 mm thick). Figures 3.1f to 3.1i are different images of this tubular gel. The tube is flexible and bendable, yet strong and robust. To our knowledge, such robust alginate tubes have not been reported in the literature.

The above technique is general and can be modified in many ways. First, it is not limited to Ca^{2+} ions. Any multivalent cation that can crosslink alginate (such as Sr^{2+}, Cu^{2+}, Fe^{3+} and Ho^{3+}) could be incorporated into the mold and used to gel alginate. Instead of alginate, other polymers that can be gelled by such cations could also be used (such as pectin or polyacrylic acid). Also, we are not limited to using agarose as the mold. If the mold does not have be to be removed, any gel, including chemically crosslinked hydrogels (e.g., acrylamides) could be used as the calcium containing mold. If the mold needs to be removed at a more moderate temperature, we can replace agarose with gelatin, since gelatin gels can be melted around 40°C. Additionally, molds of any shape and geometry can be used. Examples with disc-like molds and flat-sheet molds are shown below and in all cases, the alginate gel forms around the mold.

3.3.2 Kinetics of Gel Growth

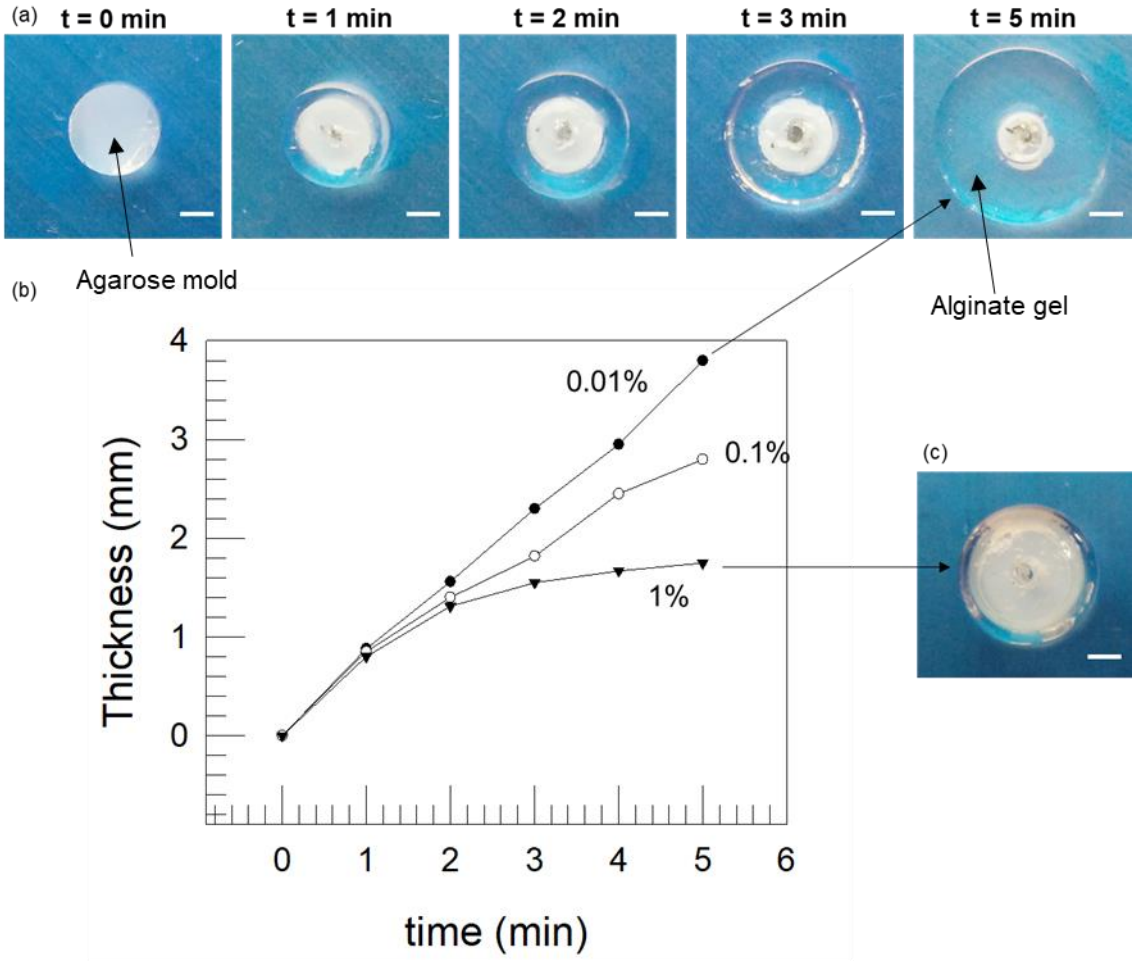

Figure 3.2. Kinetics of gel growth. (a) At t = 0, 10 V is applied across the set-up. The sequence of images shows the growth of the alginate gel around a disk-shaped agarose mold containing 0.01 wt% Ca^{2+}. Scale bar: 2 mm. (b) Plot of thickness of the alginate gel with time for three Ca^{2+} concentrations: 0.01, 0.1 and 1 wt%. (c) Photo of the alginate gel for the case of 1 wt% Ca^{2+} after 5 min at 10 V.

We studied the growth of the alginate gel with time around an agarose mold for different Ca^{2+} concentrations in the mold. For this, the agarose mold was made in the shape of a disk (5.5 mm in diameter, 4 mm in thickness) and placed in a petridish (refer experimental section for details) while being observed under an inverted microscope.

Figure 3.2a shows images of the growing alginate gel over 5 min at a voltage of 10 V. These images are for the case of 0.01 wt% Ca^{2+} in the agarose mold. The alginate gel can be easily resolved because it is transparent while the agarose mold is cloudy. The thickness of the alginate gel steadily increases over time, with the increase being approximately linear, as shown by the plot in Figure 3.2b. However, as the Ca^{2+} concentration is increased, a different shape of the plot is seen: after an initial linear increase, the gel thickness saturates within the 5 min period. Figure 3.1c shows that, after 5 min, the alginate gel for the case of 1 wt% Ca^{2+} is ~ 2 mm thick whereas it is ~ 4 mm thick for the case of 0.01 wt% Ca^{2+}.

The above result might seem counterintuitive at first. One would expect the thickness to increase with higher availability of Ca^{2+} ions. However, the opposite is observed in our experiments. We hypothesize that there is a difference in the mode for gel formation at low and high Ca^{2+} concentrations, as depicted in Figure 3.3. At high Ca^{2+} concentrations, we expect the ions to crosslink the alginate into a dense network, which could hinder further migration of Ca^{2+} ions from the interior of the mold, and thereby restrict the thickness of the gel. In contrast, the network at lower concentrations of Ca^{2+} is expected to be less dense, allowing Ca^{2+} ions to migrate through, and thereby leading to much thicker gels. Our results thereby suggest that there are advantages to using relatively low Ca^{2+} (0.01 to 0.1 wt%) in the mold. That is, the gels can grow to larger dimensions, as discussed above. A second advantage at these lower Ca^{2+} concentrations is that there is no significant growth of the gel in the absence of electrical signals; thus, we have a true "on-off" switch for gel growth. The gel grows only when the electrical signal is on and the

growth stops when the signal is turned off. In contrast, when the Ca^{2+} is higher than 1 wt%, a thin gel layer forms slowly around the mold even in the absence of the field because sufficient Ca^{2+} can simply diffuse out of the mold. (A comparison of gels formed with and without the electrical stimulus is provided below.)

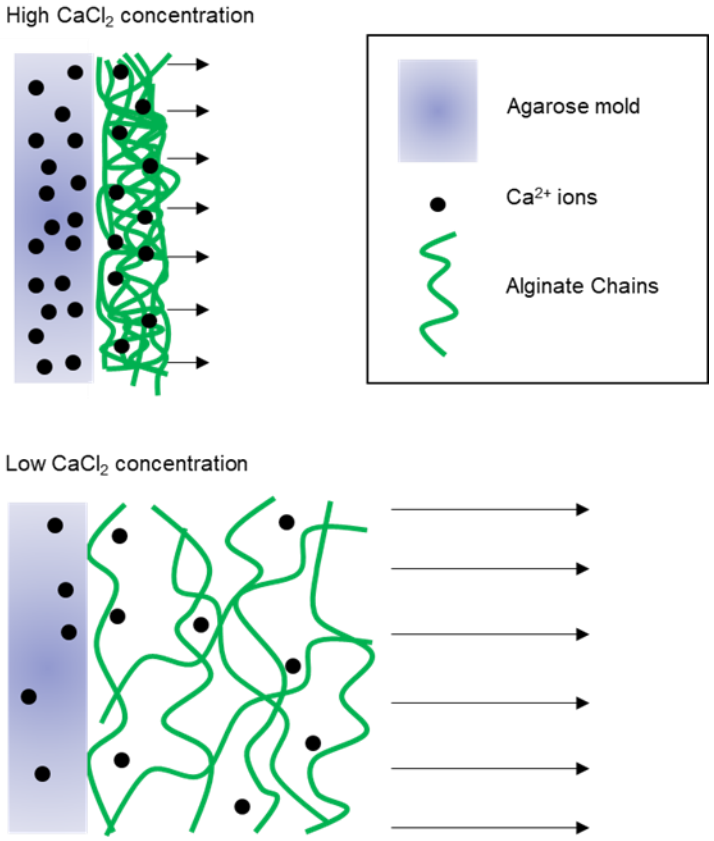

Figure 3.3. Schematics illustrating differences between the alginate gels formed at different Ca^{2+} concentrations. At high Ca^{2+} concentrations, the alginate is crosslinked into a dense network, which hinders migration of Ca^{2+} ions and thereby producing thinner gel. On the other hand, at lower Ca^{2+} concentrations, the alginate is crosslinked loosely, allowing for farther migration of Ca^{2+} and producing a thicker gel.

We also observed that when the concentration of Ca^{2+} is low (< 0.5 wt%), the agarose gel mold shrinks during the electro-gelation process. For example, the disk-shaped agarose in Figure 3.2a (containing 0.01 wt% Ca^{2+}) shrunk from 5.5 to ~ 3 mm in 5 min.

Such shrinkage is not seen at 1 wt% Ca^{2+} as can be noted from Figure 3.2c. We believe that the shrinking is due to the stresses exerted by the charged alginate gel on the agarose. That is, alginate chains in a low-Ca^{2+} gel would still retain sufficient anionic character and therefore attempt to move electrophoretically toward the anode, and this would exert a compressive stress on the central agarose. At higher Ca^{2+}, the alginate chains in the gel would have negligible residual charge, and therefore would not have the same electrophoretic tendency.

3.3.3 Effect of Ca^{2+} Concentration on Gel Properties

Next, we studied the effects of Ca^{2+} concentration in the agarose mold on the alginate gel properties (specifically, the rheological properties). In all cases, alginate gels were allowed to form for 5 min at 10 V around a cylindrical agarose mold, and thereafter, the gels were peeled off from the mold, cut into discs of diameter 20 mm, and tested on a rheometer. Figure 3.4a shows a plot of G' (elastic modulus) of the alginate gel vs. Ca^{2+} concentration. The red curve corresponds to the 10 V bias and the black curve to no voltage. Note that there are no black data points below 1 wt% Ca^{2+} because no gel is formed without an electrical signal under these conditions, as mentioned earlier. For the 10 V case, G' increases sharply as the concentration of Ca^{2+} increases. No significant change in G' is observed for the gels formed by simple diffusion (no voltage), regardless of the Ca^{2+} concentration. This is a significant finding as it means that the electrical signal offers better control over the gel properties. The frequency sweep (Figure 3.4b) and stress sweep (Figure 3.4c) are shown for alginate gels formed at 10 wt% Ca^{2+} by electrical signals and by simple diffusion. Both gels show elastic rheology ($G' > G''$, moduli nearly independent of

frequency), but the magnitude of G', which reflects the gel stiffness, is about 10-fold higher for the electro-formed gel. Both gels are shear-sensitive to approximately the same extent, i.e., in both cases the moduli sharply drop at moderate strains (~ 1–10%).

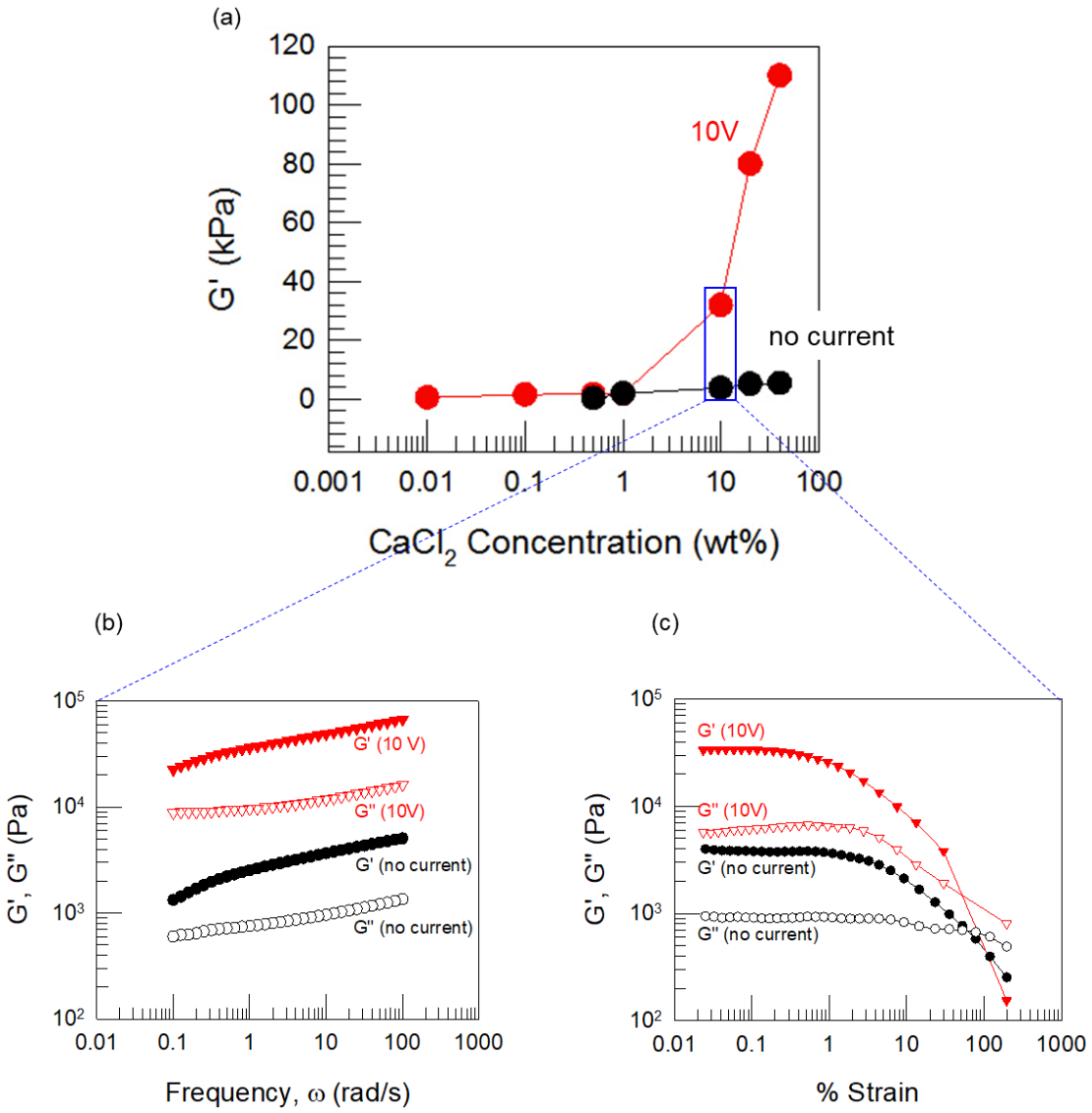

Figure 3.4. (a) Elastic modulus G' of alginate gels formed at various Ca^{2+} concentrations in the agarose mold. Red curve corresponds to the case with 10V bias and black curve corresponds to the case with no bias. Bottom plots show frequency sweep (b) and stress sweep (c) for 10 wt% $CaCl_2$.

3.3.4 Effect of Applied Voltage

Next, we varied the applied voltage to see its effect on gel formation. These tests were performed with agarose molds containing 0.1 wt% Ca^{2+}. All other parameters were kept constant. Figure 3.5 shows the thickness of the alginate gel after 5 min at specific voltages. We see that the thickness is zero at < 1 V, then increases with increasing voltage, and finally saturates around 20 V. The increase in gel thickness with voltage is expected because a higher voltage increases the electrophoretic mobility of Ca^{2+} ions, allowing the ions to migrate farther from the mold and hence gel a larger volume of alginate chains.

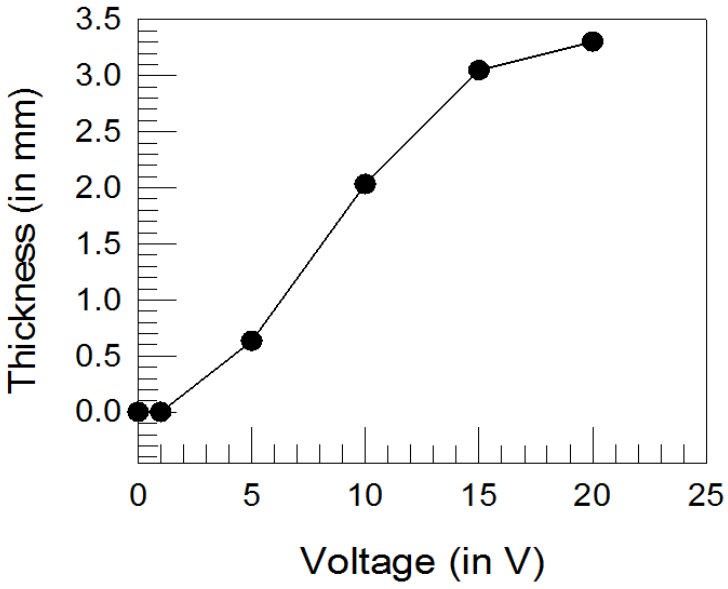

Figure 3.5. Thickness of the alginate gel vs. applied voltage. The data correspond to a concentration of 0.1 wt% Ca^{2+} in the agarose mold and the thickness was measured after applying the voltage for 5 min.

3.3.5 Branched Alginate Gel Tubes

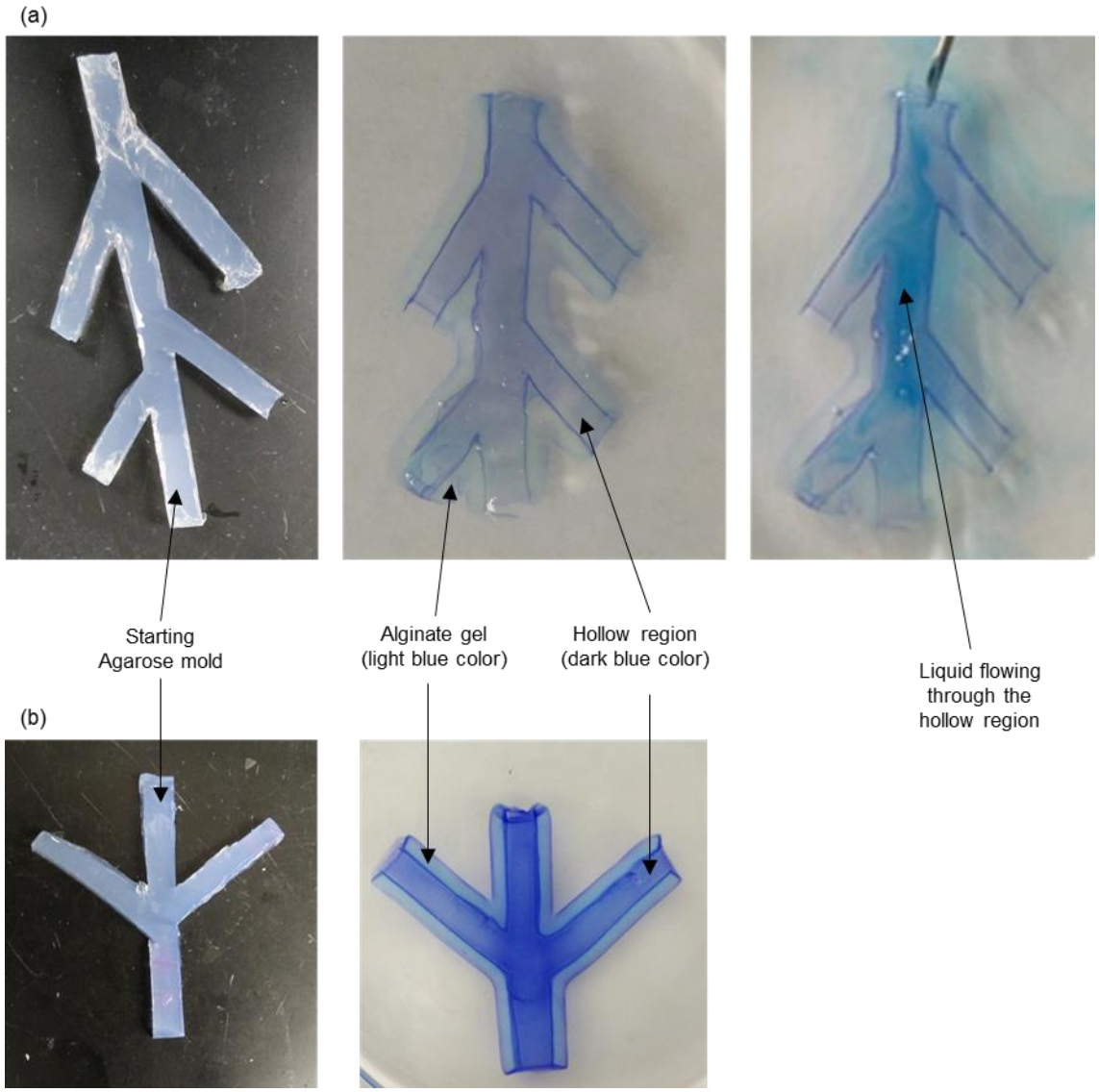

Figure 3.6. Branched alginate gel tubes. Images on the left show the solid agarose mold filled with Ca^{2+}. Images in the center show the corresponding hollow alginate gel tube. The image on the right in (a) depicts water flowing through the tube. The dark blue colour in (b) is obtained after flowing water with methylene blue dye through the tube.

Our use of a thermo-responsive mold as a source of multivalent cations allows us to realize alginate gels in complex geometries that are difficult to form through traditional methods. One possibility is branched tubes, as shown in Figure 3.6. We first made agarose

molds having solid, but branched structures, and loaded with 1 wt% Ca^{2+}. These were placed in 1 wt% alginate solutions and left to stand for 2 h without applying a voltage (i.e., in this case, we relied on diffusion of Ca^{2+} out of the mold to form the interfacial alginate gel). Thereafter, the ends were cut and the structures were placed in a hot water bath to remove the agarose. The resulting hollow, branched alginate tubes are shown in Figure 3.6, with each branch having an inner diameter of ~ 10 mm and a tube wall of ~ 4 mm. These tubes are robust enough to allow the flow of liquid through them.

3.3.6 Multiple Alginate Gel Layers with Distinct Payloads

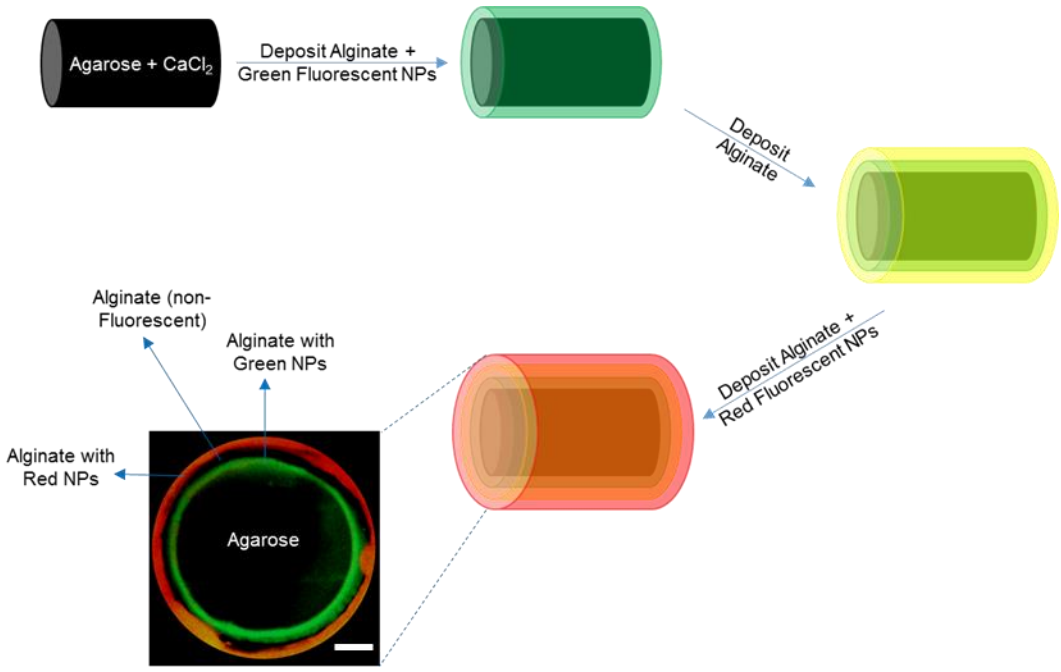

Figure 3.7. Synthesis of multiple concentric layers of distinct alginate gels around an agarose mold. Electrical stimuli are used to coat a Ca^{2+}-containing cylindrical agarose mold with successive layers of alginate gels containing (1) green-fluorescent NPs; (2) no NPs; and (3) red-fluorescent NPs. A fluorescence micrograph of the tube cross-section (overlay of green and red fluorescence) shows the multiple layers of the structure. Scale bar: 1 mm.

Our inside-out technique, i.e. gelation starting from the core and extending outward, can be used to grow sequential alginate gels. This can be used to form concentric multilayer structures, as shown in Figure 3.7. We have incorporated fluorescent nanoparticles (NPs) in each layer to distinguish them. First, a cylindrical agarose mold with 0.1 wt% Ca^{2+} was created. This was placed in an alginate solution (1 wt%) that contained dispersed green-fluorescent NPs (0.5 wt%). A voltage of 10 V was applied for 30 s to form the first alginate gel layer (we expect the NPs to be immobilized in the gel). This procedure was then repeated with a second alginate solution with no NPs, and finally with a third alginate solution containing red-fluorescent NPs (0.5 wt%). The fluorescence micrograph of the final cross-section shows the green-colorless-red sequence of alginate layers (from the center proceeding outward), as expected. Note that this process can be extended even further. As long as there are Ca^{2+} ions left in the agarose core, we can grow a fresh alginate gel layer on the periphery.

The above technique is versatile and rapid. Each layer was formed in just 30 s, and thus it is possible to rapidly build multiple, distinct layers. Any payload, such as colloidal particles or enzymes that are present in the alginate solution will also get incorporated into the corresponding alginate gel. Also, the entire process can be done under mild and biologically benign conditions, i.e., the alginate can be dissolved in a physiological buffer and the temperature can be maintained at 25 or 37°C. To illustrate the biocompatibility of our technique, we show the encapsulation of bacteria (*E. coli*) in an alginate gel layer. The *E. coli* used here were genetically engineered to express green-fluorescent protein (GFP) as they metabolized. Pellets of these *E. coli* (0.5 wt%) were combined with the alginate (1

wt%) in phosphate buffered saline (PBS). A cylindrical agarose mold with 0.1 wt% Ca^{2+} was placed in the above sample and a voltage of 10 V was applied for 3 min (Figure 3.8). The structure was then removed and placed in media for the bacteria to grow. The fluorescence micrograph of the cross-section shows the green fluorescence from the GFPs in the alginate gel layer, indicating that the bacteria are able to grow in the gel.

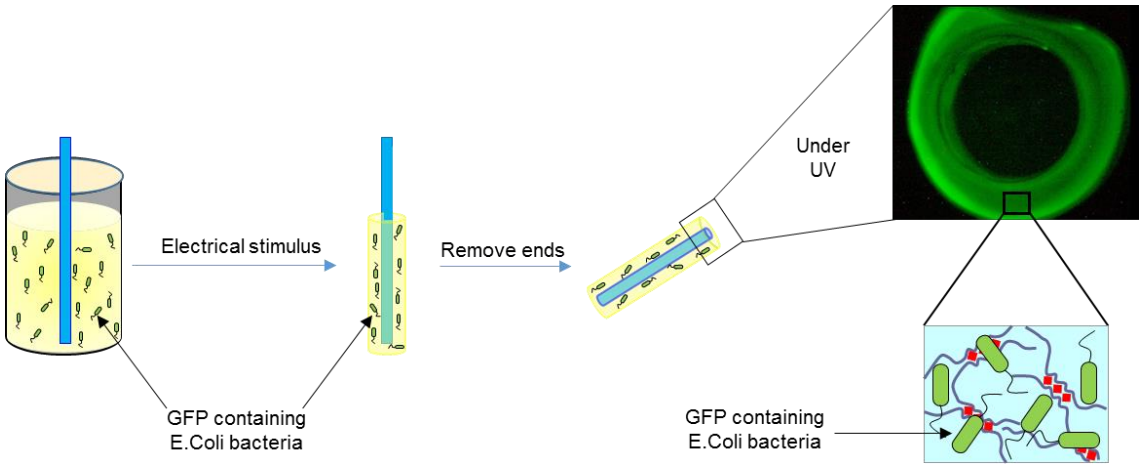

Figure 3.8. Encapsulation of *E. coli* in an alginate gel layer. GFP-expressing *E. coli* are mixed with an alginate solution, and an electrical stimulus is used to form a gel from this solution around an agarose mold. The fluorescence micrograph shows the green colour of the alginate gel layer, confirming the presence of *E. coli* in this layer.

3.3.7 Growth of Alginate Gels in Specific Patterns on Flat Surfaces

In the above experiments, the alginate gel is electro-formed everywhere around the original agarose mold. We now show that, by using a hydrophobic coating on the mold, we can dictate the gel growth to occur only in specific regions. For this proof of concept, we have used a commercially available coating ("Rust-Oleum Never-Wet spray), which has to be applied in a two-step process. We start with a flat sheet of agarose containing 0.1

wt% Ca^{2+} with dimensions of 6 cm × 1 cm and a thickness of 8 mm. The hydrophobic coating was applied selectively over a central portion of the sheet (1.2 cm wide, extending across the width), as well as to the edges of the sheet, as shown in Figure 3.9, top. When the voltage is applied, the alginate gel (pink color in the figure due to acid red 52 dye) grows vertically over the regions not covered by the hydrophobic coating. Over the rest of the mold, the coating prevents the Ca^{2+} ions and the alginate chains from contacting each other to form a gel.

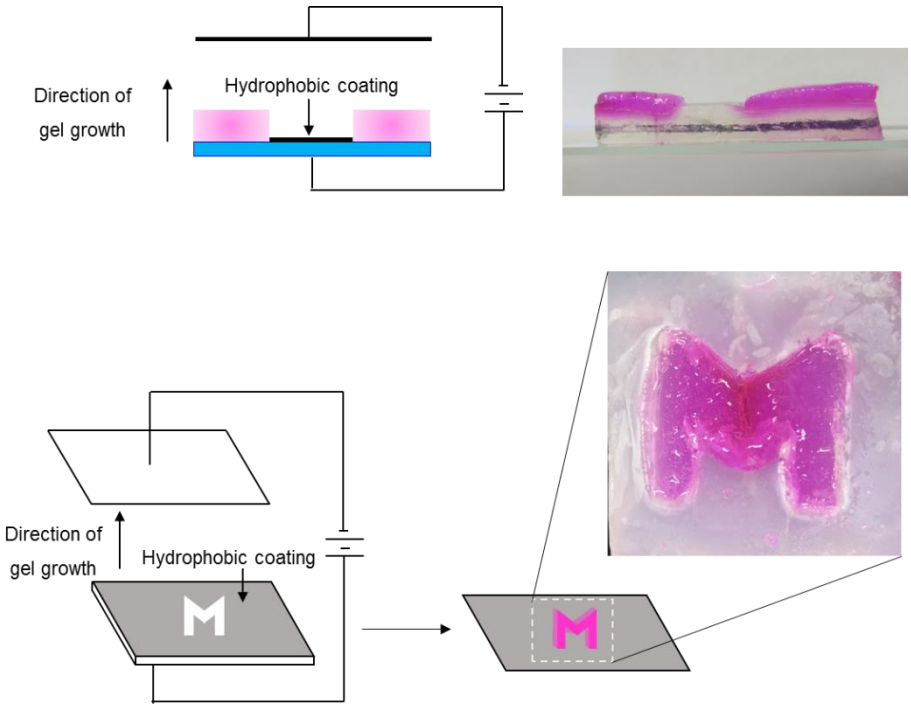

Figure 3.9. Selective electro-deposition of alginate gels. A commercial hydrophobic coating on the agarose mold restricts the growth of alginate gel to the uncoated regions. This aspect can be seen from both the images. In the top case, the gel (pink) grows vertically on the two side strips but not on the coated central strip. In the bottom case, the coating is applied everywhere on the flat mold except on the region corresponding to the letter "M". This leads to the alginate gel being in an "M" pattern.

Next, we demonstrate the patterned growth of alginate gels using the same hydrophobic coating. We cut aluminium foil in the shape of the letter “M” and placed this on the agarose mold (Figure 3.9, bottom). The hydrophobic coating was then sprayed onto the mold. When the foil was removed, the mold was covered with the coating everywhere except for the “M” region. The presence of the coating can be verified from the fact that water does not wet the coated region, i.e., the contact angle of water drops placed on this region exceeds 90°. Next, the voltage was applied for 5-7 min and we see that the alginate gel selectively grows only on the uncoated region, i.e., in the pattern of the “M”. The feature sizes in the pattern here are ~ few mm, but finer feature sizes can be obtained by using lithographic masks and also with a more sophisticated coating.

3.4 Conclusions

We have described a new technique to develop hollow alginate gel structures that are generally not possible through traditional methods. Calcium containing agarose gel mold is placed in an alginate solution and electrical bias is applied. The oppositely charged species move towards their respective electrode and gets crosslinked upon contact to form flexible, robust, and transparent gel. We have shown that lower concentration of calcium inside the agarose gel gives rise to a thicker gel and since no significant gelation occurs at this low concentration without the electrical stimulus, it provides us a control over the gelation process. We have also demonstrated the utility of our system in developing multilayered structures and encapsulation of biological species. Finally, we have illustrated the development of patterned gels is also possible with the aid of commercially available hydrophobic coating.

Chapter 4

Electrically Induced Rupture of Microparticles

4.1 Introduction

Delivery systems that require payload release at a specific site, specific time, and at a controlled rate have tremendous applications in drug delivery and directed catalysis applications.[35] To overcome the limitations of traditional delivery systems, researchers are trying to develop new materials that can "sense" their environment and respond accordingly. Different stimuli, such as pH, light, temperature, ultrasound etc. have been investigated in this regard.[36] A new and intriguing stimulus is the electric field.[6,37-41] Electric fields can be directed to a very specific site, and electrical responses are usually quite fast. However, typical materials that are sensitive to electrical stimuli tend to be based on intrinsically conducting polymers (ICPs) like polypyrroles and polythiophenes, which have their limitations.[7,39,42] These include the facts that ICPs are rather expensive, require synthesis by complicated procedures, and are generally not biodegradable. Also, the ICPs need to be in direct contact with electrodes to respond, which may not always be practical. Additionally, only payloads with appropriate oxidation or reduction potential can be released from ICPs. In addition to ICPs, electrical responses have also been studied for polyelectrolyte hydrogels, as described in Chapter 2.[5,43] Most of these hydrogels are formed by the chemical crosslinking of synthetic monomers. In these cases, the gels are not conductive to electrons, but to ions. Responses can occur even when the electrodes are placed far away from the gels, but generally, the response is limited to changes in gel volume (swelling or shrinking), or the bending of gel filaments.

In this chapter, we describe the response of polymer microparticles under electric fields. Specifically, we show that these microparticles deform and break under an electrical stimulus. To the best of our knowledge, this is the first time such observations have been reported. These microparticles are synthesized through a simple one-step process involving electrostatic complexation of a charged polymer with multivalent ions (or a surfactant or a second polymer) of the opposite charge. The typical polymers we use are well-known biopolymers like alginate and chitosan, which are biocompatible, biodegradable, and extensively used in biomedical applications. Moreover, the microparticles made from these polymers can easily encapsulate any type of payload. These payloads will be released when the microparticles are ruptured; thus, our system could be useful for drug delivery. Another aspect is that the particle rupture can be triggered remotely by the electric field, i.e., electrodes do not have to be in direct contact with the particles during this process. The mechanism for particle rupture is non-trivial, and we discuss the various possibilities that can explain it.

4.2 Experimental Section

Materials and Chemicals. Alginate (medium molecular weight, viscosity >= 2000 cP, 2%), Chitosan (medium molecular weight, 190–310K; degree of deacetylation ~ 80%), Copper (II) chloride dihydrate, glutaraldehyde solution (grade I - 50% in water), and Rhodamine B were obtained from Sigma-Aldrich. Sodium dodecylbenzenesulfonate (SDBS) was purchased from TCI America. Thin graphite sheets were purchased from Saturn Industries. Green fluorescent latex nanospheres (diameter ~ 100 nm) were

purchased from Polysciences Inc. Carbon black particles (N110) were purchased from Sid Richardson Carbon Company. All chemicals were used as received.

Solution Preparation. Alginate solution was prepared by dissolving 2 wt% alginate in deionized water (DI). Chitosan solution was prepared by dissolving 2 wt% chitosan in 0.2 M acetic acid solution. For beads containing carbon black, 0.25-0.5 wt% carbon black was mixed with alginate and the solution was sonicated for one minute to better disperse the carbon black. For fluorescent capsules, green fluorescent latex nanospheres were suspended in the biopolymer solution.

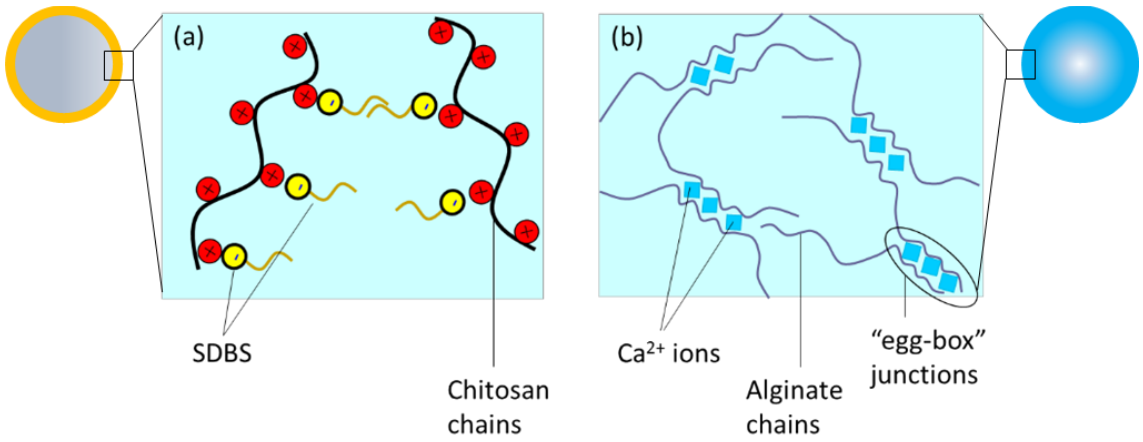

Figure 4.1. Two kinds of microparticles formed by physical crosslinking of biopolymers by oppositely charged molecules. (a) Chitosan microcapsules. Here, the shell is formed by crosslinking of the cationic chitosan by the anionic surfactant SDBS. (b) Alginate microbeads. Here, the anionic alginate is crosslinked by divalent Ca^{2+} cations.

Capsules / Beads Fabrication. Droplets of 2 wt% alginate solution was dropped slowly into a stirring solution of 8 wt% $CuCl_2$. The size of the beads is dictated by the size of the drop they are formed from. The size of the drops was varied by using either plastic transfer pipettes or needles of different gauges. Cu^{2+} ions crosslinks Guluronic (G) parts of alginate

through egg-box junctions to form these beads (Figure 4.1b). The incubation time in $CuCl_2$ was around 2 min. The beads were then washed and stored in 10 mM NaCl solution. Chitosan-SDBS capsules were formed in an analogous way. 2 wt% chitosan solution was added dropwise into a stirring SDBS solution (5 wt%). Figure 4.1a depicts the crosslinking of positively charged chitosan with negatively charged SDBS. The capsules were incubated for 3-5 min and washed with DI water. The capsules were stored in 10 mM NaCl solution.

Microparticles: Figure 4.2b shows the microfluidic setup used in this study for forming microcapsules and microbeads. This setup was developed in our lab previously and has been described in more detail elsewhere.[44] It allows for the generation of microscale aqueous droplets at the tip of a capillary. A key distinguishing feature of this method over other microfluidic methods is that we do not use an immiscible oil phase to form the aqueous droplets. Instead, pulses of compressed air or nitrogen gas is used to shear off the droplets from the capillary tip. To generate these pulses, we connect a gas-flow controller to a function generator. The gas flows as a sheath around the tip of an inner glass capillary of diameter of about 100 – 200 μm in which an aqueous solution is flowed (the liquid flow is controlled by a syringe pump). For every pulse of gas, an aqueous droplet is dislodged from the tip of the inner capillary. The flow rate of the liquid as well as the frequency of the pulsing gas dictate the volume of the liquid droplet. Droplets generated by this technique are very uniform, with polydispersities of <3% in their diameter.[44]

For alginate beads, 2 wt% alginate solution was flown through the inner capillary and the droplets were sheared off into 8 wt% $CuCl_2$ solution and allowed to incubate for 2 min.

The beads were then washed and stored in 10 mM NaCl solution. (Consistent with the literature, we refer to these alginate particles as beads rather than capsules because they are expected to be uniformly cross-linked rather than having a core−shell structure).[45,46] For chitosan capsules, we used the device to shear off 2 wt% chitosan micro-droplets into 5 wt% SDBS solution. After incubating for 3 min, the capsules were washed and stored in 10 mM NaCl solution.

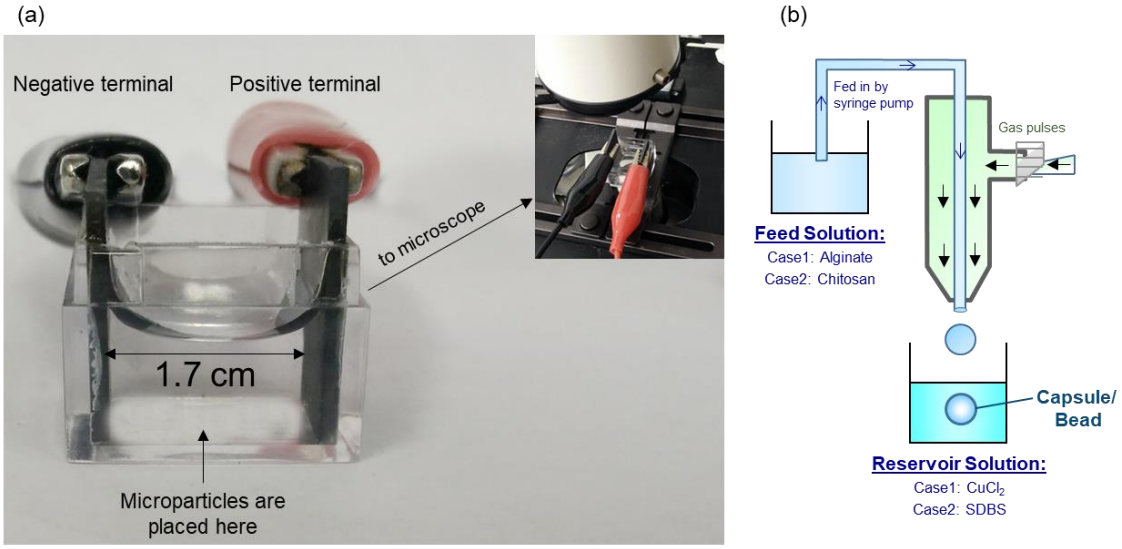

Figure 4.2. (a) Experimental set-up to test electro-response of microparticles. Graphite electrodes are positioned 1.7 cm apart inside a transparent cubical box and are connected to the power source. 3 mL of the electrolyte is placed in between the two electrodes. Inset image shows the set-up placed on an inverted microscope for optical monitoring. (b) Preparation of microparticles using a pulsed-gas flow device. The feed solution is pumped through a microcapillary, at the end of which they are sheared off into microdroplets by pulsed N_2 gas. The droplets are collected in a reservoir solution where they are physically crosslinked into microparticles.

Experimental Set-up. Figure 4.2a shows the photo of the test cell. It comprises of a transparent cubical box (~ 2 cm × 2 cm × 2cm) and two planar graphite electrodes. The graphite electrodes were separated by 1.7 cm. The test cell was filled with 3 ml of

electrolyte. The assembly was placed under an inverted microscope (Zeiss Axiovert 135 TV) for optical monitoring (inset in Figure 4.2a). A DC power source (Agilent E3612A) was connected to the two electrodes and a bias of 15V was applied across the test cell. Gel bending experiments and experiments with macro-beads were performed in a petridish instead of the test cell. 40 ml of the electrolyte was used. The electrodes were separated by 9 cm and a bias of 80V was applied.

Fluorescent Microscopy. Images of capsules containing green fluorescent particles were taken on Zeiss Axiovert 135 TV microscope using a band pass excitation filter (450-490 nm) and a band pass emission filter (515 - 565 nm). Images were analysed using ImageJ software.

Cu^{2+} - Alginate Hydrogel Preparation. 1 ml syringes were filled with 2 wt% alginate and stored at -18°C until frozen. These solidified solutions were dropped in $CuCl_2$ solution for different incubation times. After washing with DI water, the gels were stored in 10 mM NaCl solution.

4.3 Results and Discussion

4.3.1 Electrical Rupture of Beads and Capsules

We studied the behavior of Cu^{2+}-crosslinked alginate microbeads (200 μm radius) under an electric field using the setup shown in Figure 4.2 (this is schematically shown in Figure 4.3). A specific bead is placed in a 10 mM NaCl solution as shown in Figure 4.2a and observed under an optical microscope. Figure 4.3 shows the behavior of the beads when a voltage of 15 V is applied across the test cell. The anode (positive electrode) is on the left of the bead and the cathode (negative electrode) is on the right. The two sets of images are for the cases when the beads are made without carbon black (CB) particles (top) and with 0.5 wt% of dispersed CB (bottom). The CB particles can be considered a model payload and their presence aids in visualization. Within 100 s of the voltage being applied, we observe that the bead *swells* on its left side, which is the side near the anode. The swelling can be clearly seen in Figure 4.3b because of the dilution of CB in the left side of the bead (i.e., this side looks much more transparent). Thereafter, we observe that the left side of the bead ruptures, and this process is complete within 120 s. The final collapsed structure looks like a deflated balloon in Figure 4.3a. In Figure 4.3b, the rupture of the bead causes the inner payload, i.e., the CB particles, to spill out and spread all over the microscopic field of view. This observation shows that bead rupture can serve to release internal payloads.

Regarding the presence of salt in our experiments, we also studied the breaking of alginate-Cu^{2+} beads in the absence of salt, i.e., in DI water. In that case also, the beads ruptured when subjected to a voltage of 15 V, but it took much longer (> 15 min) compared

to the results in Figure 4.3. We then tested the breaking at 1 mM, 10 mM and 100 mM NaCl, but there was no systematic trend for breaking time with changing NaCl concentration. (Higher NaCl was not studied because the beads slowly disintegrate due to exchange of Cu^{2+} with sodium ions.[47]) Based on these findings, we chose to perform all further tests in a 10 mM NaCl solution.

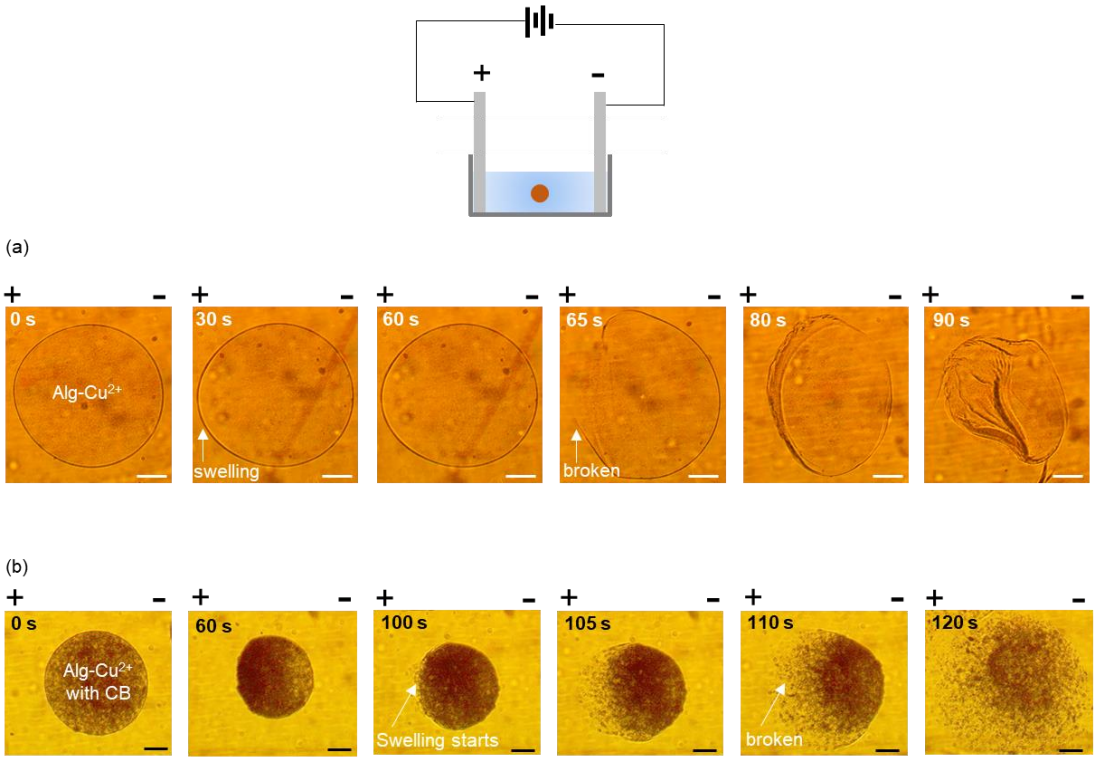

Figure 4.3. Electrical rupture of alginate-Cu^{2+} microbeads over time**.** The schematic of the setup is shown on the top. A microbead is placed in 10 mM NaCl and subjected to a voltage of 15 V. (a) Bare microbead; (b) Microbead with CB particles inside. In both cases, the bead undergoes swelling on the anode side and ultimately breaks at this side. Scale bars are 100 μm.

Figure 4.4 shows the response of a chitosan-SDBS microcapsule to the same 15 V voltage. The capsule contained 0.5 wt% of dispersed green-fluorescent microparticles, and the images were taken under a fluorescence microscope. Note that the capsule differs from

the beads in that there is a shell covers a liquid core, whereas the beads are more uniformly gelled throughout. In this case, around the 60 s mark, the left (anode) side of the capsule appears to bend and fold inward. Thereafter, at ~ 135 s, this side ruptures and the contents again spill out into the solution.

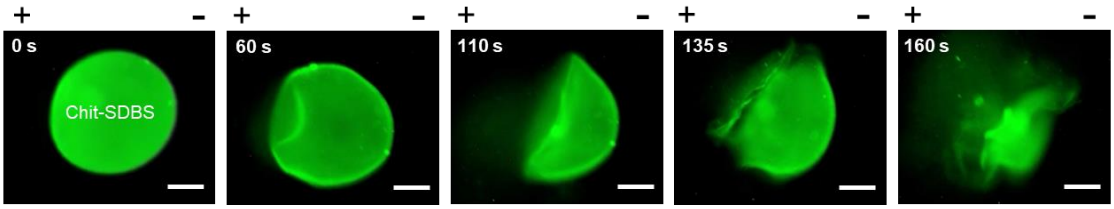

Figure 4.4. Electrical rupture of a chitosan-SDBS microcapsule over time. The setup is identical to that in Figure 4.3. The capsule contains green-fluorescent particles. Here, the capsule undergoes bending and shrinking (Images 2 and 3) at the anode side before breaking at this side (Images 4 and 5). Scale bars are 100 μm.

We conclude that electrical rupture is seen with both microbeads and microcapsules, which span two different particle morphologies and also two different chemistries (alginate is an anionic biopolymer while chitosan is a cationic one). Thus, such a response to electric fields seems to be a general phenomenon with microparticles formed by ionic (physical) interactions. We can also repeat the above experiment with multiple particles at one time, and this is shown in Figure 4.5 for the case of alginate-Cu^{2+} beads. When subjected to a voltage of 15 V, all the beads swell at their anode side and eventually break at this side within 5 min.

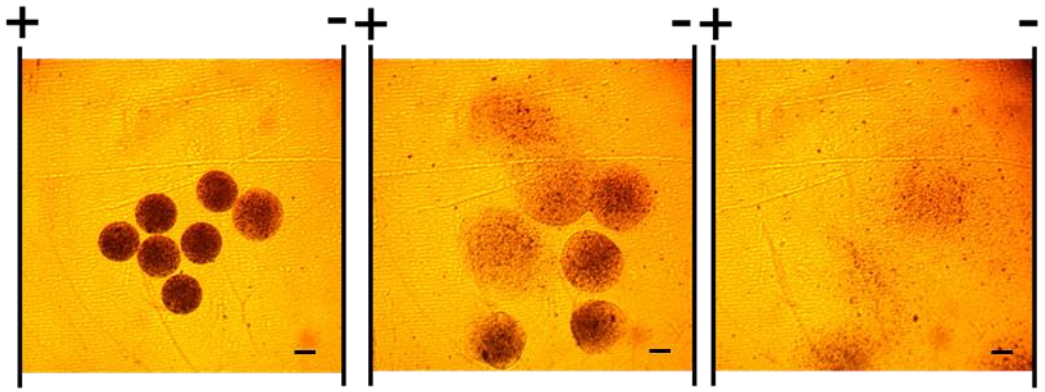

Figure 4.5. Electrical rupture of multiple alginate-Cu^{2+} microbeads over time**.** The beads are placed in 10 mM NaCl and subjected to a voltage of 15 V. All the beads swell on the anode side and then break at this side. Scale bars are 100 μm.

4.3.2 Effects of Different Variables on Bead Breaking Time

From the above data, it is possible to roughly estimate the breaking time of a given type of microparticle, i.e., the time at which we can detect the rupture by optical microscopy. We now present data on the breaking time of alginate-Cu^{2+} microbeads as a function of different variables. First, we varied the applied voltage. Figure 4.6 shows a monotonic decrease in breaking time with increasing voltage. No breaking is observed when the applied voltage is below 2 V, i.e., close to the electrochemical stability window of water. Similar results were reported in the literature for the response of hydrogels to electric fields, i.e., a threshold potential of 2-3 V was required for actuation of gels. [48-50] Also, we studied the beads under a sinusoidal (AC) field (amplitude of 15 V and frequency of 50 Hz). No swelling or breaking of the beads was observed in this case.

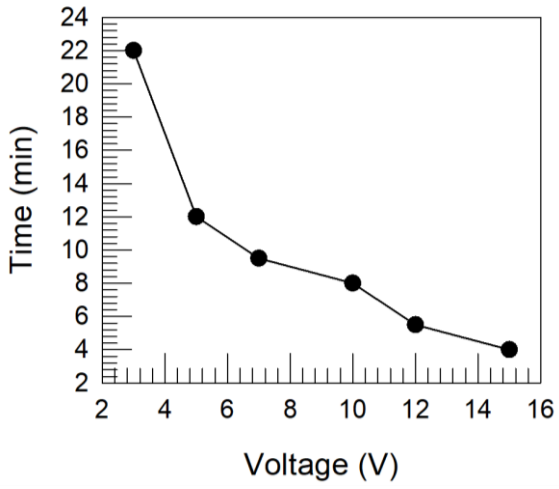

Figure 4.6. Breaking time for alginate-Cu^{2+} microbeads plotted against the applied voltage. Tests were done in 10 mM NaCl solution.

Next, we varied the parameters influencing the structure of alginate-Cu^{2+} beads. These beads are prepared by dropwise addition of 2 wt% alginate into a solution of Cu^{2+} (typically 8 wt%). As the drop stays in the Cu^{2+} solution, it gets crosslinked into a bead. The incubation time is the time the drop is allowed to sit in the Cu^{2+} solution before being washed. The higher this time, the higher the density of crosslinks between alginate chains and Cu^{2+} ions and therefore the stronger the resultant bead. Figure 4.7a shows the electrical breaking time as a function of the incubation time for beads that were otherwise identical (bead radius = 200 μm). It is clear that increasing the incubation time increases the breaking time. This result seems intuitive since stronger beads should take longer to break. We also varied the Cu^{2+} concentration used to form the beads from 1 to 16 wt%, with the incubation time fixed at 2 min. Figure 4.7b shows that the breaking time increases with increasing Cu^{2+} concentration. Again, a higher concentration of Cu^{2+} ions would be expected to make the beads more crosslinked and hence stronger, which is consistent with their taking longer to break.

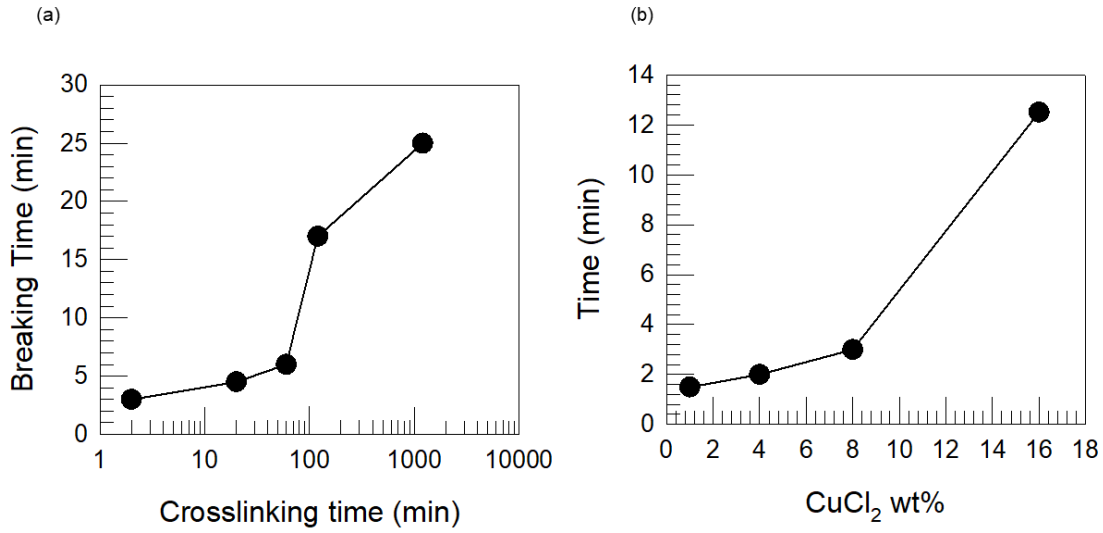

Figure 4.7. Breaking time for alginate-Cu^{2+} microbeads plotted against (a) The incubation time in 8 wt% Cu^{2+}. (b) The concentration of Cu^{2+} for 2 min incubation time. Tests were done at 15 V and in 10 mM NaCl solution.

4.3.3 Mechanism for Electrical Rupture

The crucial question from this study is why the beads and capsules break under an electrical stimulus? Analyzing electrical effects in our system is very complex and requires knowledge of concepts in polymer physics, electrochemistry, colloid science, and thermodynamics.[5,51-53] To begin our discussion, it is useful to mention one relevant behavior observed with polyelectrolyte gels, which is that the gels bend under an electric field.[51,54-56] These experiments have typically been performed with ionic gels in which the chains are chemically crosslinked. Will gel-bending be observed with physical gels such as those based on alginate? To test this, we created a cylindrical alginate-Cu^{2+} gel (see Experimental Section for details on its preparation) with a length of 4.5 cm and a diameter of 3 mm. We placed this gel in a 10 mM NaCl solution, and tested it under electric field (see Experimental section for details of the set-up). As seen in Figure 4.8a, the gel does bend under the field. The bending direction is not constant, i.e. the gel tends to change its

orientation during the experiment. Importantly, the alginate-Cu^{2+} gel does not seem to break even after prolonged exposure to the electric field. For comparison, we also prepared a macro-bead (diameter ~ 5 mm) of alginate-Cu^{2+} and tested this also under the same conditions. Figure 4.8b shows that the macro-bead breaks in a similar manner to the microbead, i.e., it swells at the anode side and then breaks at this side.

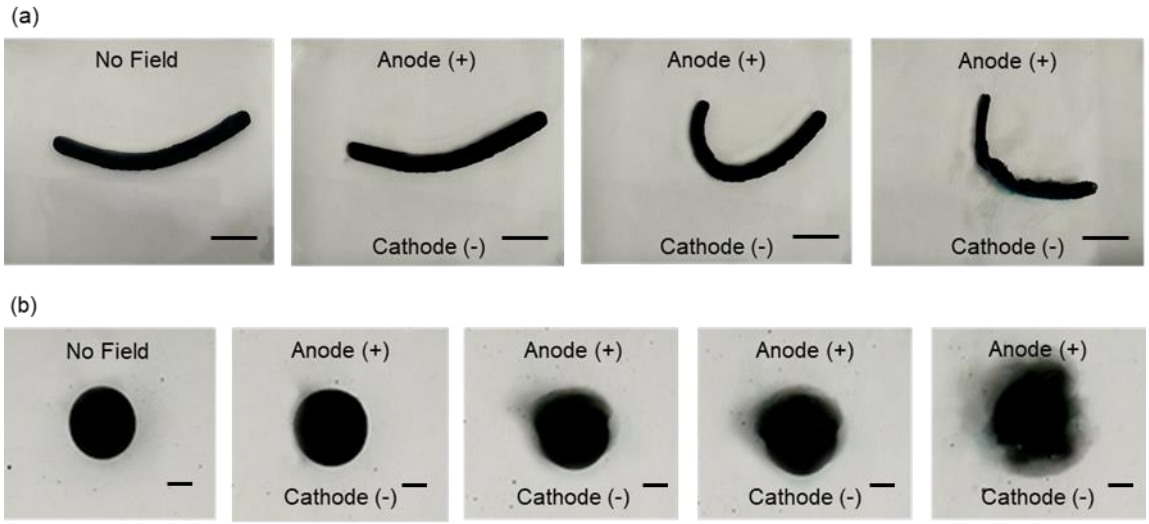

Figure 4.8. Images under an electric field of (a) an alginate-Cu^{2+} gel (with CB) and (b) an alginate-Cu^{2+} macro-bead (with CB). The gel undergoes significant bending, but does not break. The macro-bead swells on its anode side and then breaks. All experiments were conducted in 10 mM NaCl solution. Scale bar: 1 cm (gels), 2 mm (beads).

Are there spherical beads that do not break under an electric field? We have made macro-beads of the nonionic polysaccharide agarose, which are gel networks held by physical crosslinks between agarose chains. These agarose beads show no response to electric fields. Thus, the presence of residual charge seems to be a requirement for electric responses. Another observation is that microbeads formed by crosslinking chitosan with glutaraldehyde (GA) are also insensitive to electric fields. In this case, the chitosan-GA

beads are known to have a residual cationic charge, but the bonds between chitosan and GA are covalent bonds, which are much stronger than the ionic interactions in alginate-Cu2+ beads. We conclude that electrical rupture of particles only occurs when the particles are formed by weak, physical bonds of an ionic or electrostatic nature.

Now we return to the electrically induced bending of gels, which is also observed for alginate-Cu^{2+}. There are two plausible mechanisms for this.[51] The first is an electrochemical mechanism. When water is subjected to a voltage above 1.23 V, it gets electrolyzed (see Section 2.1.1).[51,57] As a result, H^+ ions are formed at the anode and OH^- ions at the cathode. In turn, this generates a pH wave in the solution (i.e., lower pH near the anode and higher pH near the cathode). When the pH wave reaches the gel, ionic groups in the gel can gain or lose their charge, which can lead to selective swelling and shrinking of the gel and thereby to gel bending. Can this explain the breaking of alginate-Cu^{2+} beads? On the anode side, we expect a lower pH, which could protonate the the carboxylates ($-COO^-$)on alginate chains. The lower charge should then cause the anode side of the bead to shrink. However, we observe the opposite behaviour, i.e. swelling at the anode side. Also, we studied alginate-Cu^{2+} beads in solutions of different pH. We observed no change at high pH while there was some shrinking of the beads at low pH. In no case was the breaking of the bead observed. All in all, an electrochemical mechanism (i.e., the attendant changes in pH) cannot explain the breaking of our beads.

Next, we consider a second mechanism for gel bending that deals with the redistribution of ions and the corresponding changes in osmotic pressure. When a charged

gel is placed in an electrolyte solution (NaCl in our case), the ions redistribute themselves according to Donnan equilibrium and in order to maintain charge neutrality. The corresponding equations are as follows:

$$C^{g}_{Na^+}.C^{g}_{Cl^-} = C^{s}_{Na^+}.C^{s}_{Cl^-} \qquad \text{Donnan Equilibrium} \quad (1)$$

$$\left.\begin{aligned} C^{g}_{Na^+} &= C^{g}_{COO^-} + C^{g}_{Cl^-} \\ C^{s}_{Na^+} &= C^{s}_{Cl^-} \end{aligned}\right\} \qquad \text{Electroneutrality} \quad (2)$$

where the superscript *g* refers to the gel and the superscript *s* to the solution. The above equations assume that the concentration of H^+ and OH^- are very low compared to the concentration of NaCl. From the two equations, it is clear that $C^{g}_{Na^+}$ will be much higher than $C^{s}_{Na^+}$ at the outset. When the voltage is applied, the mobile Na^+ and Cl^- ions will carry the current by moving towards the oppositely charged electrodes. Inside the gel, most of the current will be carried by Na^+ because of the permselectivity of anionic gels like alginate. Permselectivity is defined as the preferential permeation of one type of ion through a charged network. According to theories, the resulting movement of Na^+ ions will create differences in osmotic pressure that leads to gel bending.[5,52-54]

A similar argument may explain why our alginate-Cu^{2+} beads break under a field. The idea is that as the Na^+ ions move towards the cathode, there will be a "depletion" of Na^+ ions near the bead on the anode side and an excess of the same near the bead on the cathode side. As a result, an osmotic gradient will be created on the anode side that will cause the bead to swell (i.e., the bead will swell because there will be fewer ions outside than in the bead). This tallies with our findings. We have observed, both at the macro and

the micro scale, that alginate-Cu^{2+} beads swell at their anode side before they break. This is further shown by the schematics in Figure 4.9. We believe that, as the bead swells on one side, this side will become weaker, i.e., the chain segments will get stretched more, until the bead will eventually break on this side.

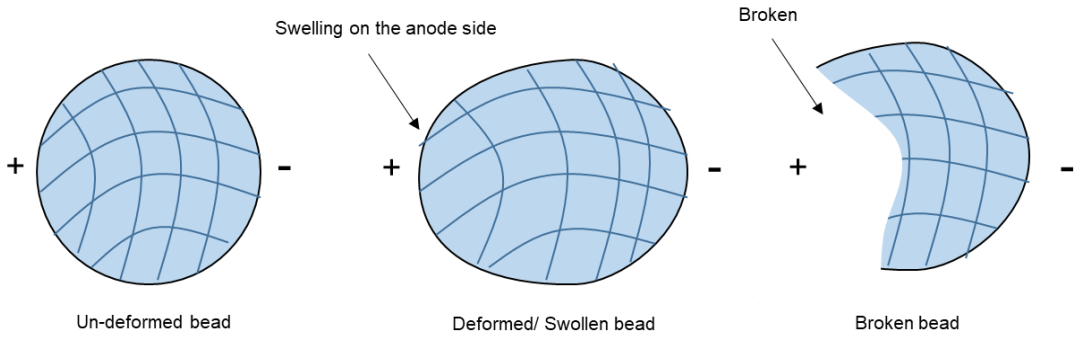

Figure 4.9. Schematics showing the breaking of an alginate-Cu^{2+} bead. When placed in an electric field, the bead swells on its anode side, making this side weaker and ultimately causing the bead to break.

4.3.4 Electro-Actuated Valves Based on Beads

Next, we illustrate an application of electrical bead rupture. We squeezed a macro-sized (4 - 5 mm) alginate-Cu^{2+} bead into the end of a plastic transfer pipette and filled the pipette with water containing a pink dye (Rhodamine B), as shown in Figure 4.10. This bead-pipette assembly is then placed in between electrodes. The setup is filled with 10 mM NaCl solution. No mixing of the fluids is observed at the outset, prior to applying a voltage because the bead is blocking the flow. When a bias of 15 V is applied, the bead deforms and breaks within about 3 min. This removes the block and allows the pink solution to flow and mix with the colorless NaCl solution. Essentially, we have created an electro-actuated

valve in this way. Interestingly, if the bead is not fit very snugly in the pipette, it can still block the flow), but even a slight deformation caused by the field can dislodge the entire bead from the pipette end and thereby allow the pink solution to rapidly flow down.

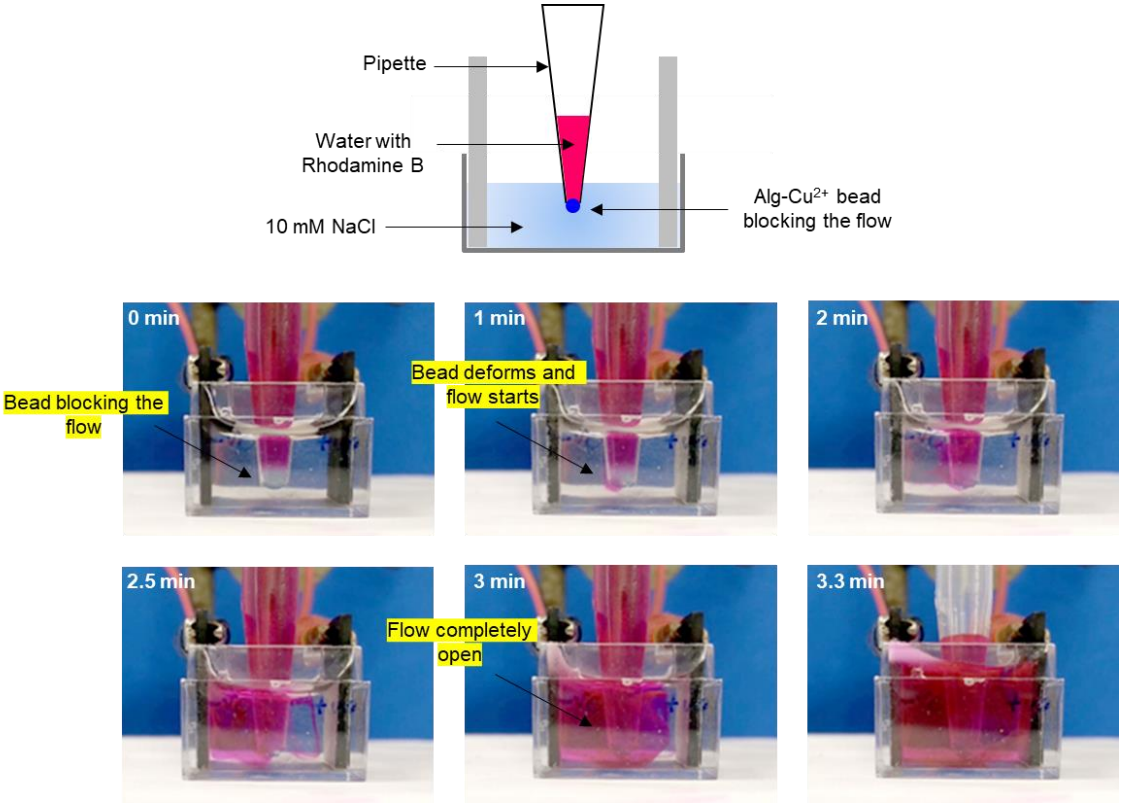

Figure 4.10. Electro-actuated valve. Alg-Cu^{2+} bead is placed at the end of a transfer pipette to block the flow of rhodamine water. The assembly is placed in between two electrodes. Schematic of the set-up is shown on the top. When electric field is applied, the Alg-Cu^{2+} bead gets deformed and broken, thereby allowing the rhodamine water to flow.

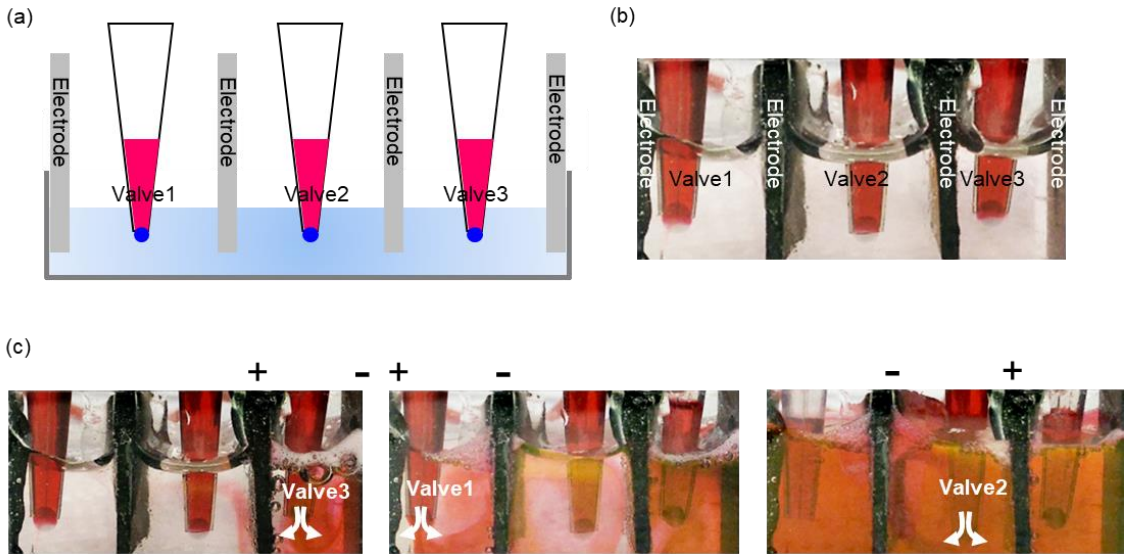

Figure 4.11. Sequential flow from multiple valves. Electro-actuated valve from Figure 4.10 is extended to include multiple valves. (a) and (b) shows the schematic and photo of the actual setup. (c) Three valves are opened sequentially in the desired order, valve3 followed by valve1 and then valve2. This experiment demonstrates the efficiency of electrical stimulus in providing spatial control.

We further extended our valve design to incorporate three valves. The schematics in Figure 4.11 show the positions of the valves and the electrodes in the setup. Again, no flow is observed initially. We then apply a voltage of 15 V across Valve 3, which ruptures the bead blocking the flow, thus "opening" the valve and allowing the red (Rhodamine 6G in water) fluid above this valve to mix with the reservoir. The other two valves are still intact at this stage. Next, we applied 15 V across Valve 1. This causes the flow to start through this valve. Valve 2 is still closed at this point. Finally, we apply 15 V across Valve 2 and induce this valve to also open. The above sequential opening of valves demonstrates several concepts that could make such a system useful for drug delivery applications. The valves here correspond to doses of drug. We can administer one dose at a time at regular intervals, or if a higher dose is desired, we can open multiple valves at the same time. Also,

our setup shows how an electrical stimulus can be directed at a precise location, i.e., we can actuate one valve without affecting the others. Other stimuli like temperature, and pH are more challenging to direct towards a precise location.

4.4 Conclusions

We have designed and demonstrated an electro-responsive release system on micro and macro scale. We believe that ours is the first system that is based on electrical responsiveness of physically crosslinked biopolymers. Our synthesis method involves dropwise addition of biopolymers to oppositely charged solution to form beads and capsules through simple physical crosslinking. The single step fabrication process would be a great advantage for mass production. Once these beads are fabricated and equilibrated in an electrolyte solution, they can be remotely triggered by applying electrical stimulus. We have studied their response by changing physical parameters like applied voltage, crosslinking ion concentration and crosslinking time. We have also discussed plausible mechanism that might be responsible for the breaking response of the beads under electric field. We have utilized the electro-actuation to demonstrate valving application by triggering a flow using electrical signal. By regulating the flow through multiple valves, we have illustrated the superior spatial control that electrical stimulus offer.

Chapter 5

Electrically Induced Adhesion of Beads to Gels

5.1 Introduction

Hydrogels are cross-linked network of polymer chains swollen in water.[1,58] They are routinely investigated by researchers because of their unique properties.[59,60] Being made of up to 90% water, they still have solid like consistencies and can withstand considerable stress.[61,62] These properties have paved a way for hydrogels to be considered for applications like tissue engineering,[63,64] bio-mimicry,[65] and cell culture studies.[66]

Although the presence of large amount of water makes hydrogel attractive for many biological applications, it presents some disadvantages as well. For example, the increase in water content generally makes the hydrogel weak, floppy, and slippery. Adhesive properties of hydrogels are also greatly affected by the presence of water.[67] Adhesion of hydrogels are particularly important because of their applications as sealants and glues, adhesive drug delivery patches, tissue scaffolds, and hemostasis and surgical sealants. Moreover, biomimicking gel-like bodies of aquatic creatures (such as squids and jellyfish) or land creatures (such as worms) require combining gels of different geometries, properties, and chemistries into one structure. There have been many successful attempts to make sticky and adhesive hydrogels.[68,69] Self-healing hydrogels have been designed that can repair themselves upon damage.[70] Several hydrogels have been realized that have excellent sticking properties to different substrates.[62,71]

There are three prevalent issues with these adhesions of hydrogels. 1) They require specific chemistries to be adhesive, which might not be practical for hydrogels with different applications;[62] 2) they require large area of contact for good adhesion, which pose problems when adhesion involving spherical geometries is required; and 3) the time scale for these adhesions is quite long.[72,73] There are some studies where one or two of these problems are addressed.[74] However, research on hydrogel adhesion techniques that addresses all of these issues is quite rare.

One particular technique that is important in this regard involves adhesion induced by electric field.[75,76] Authors have shown that two oppositely charged chemically crosslinked polyelectrolyte hydrogels can be adhered by the application of a directional electric field. They have also designed hydrogel constructs that can be remolded into different flat shapes or can be used to repair damaged hydrogels.[77,78] This technique is particularly impressive because the time scale required for adhesion is quite small, i.e. of the order of a few seconds. The system, involving contact interface of oppositely charged polyelectrolytes, itself is important due to applications in electronics[79] and multilayer assemblies.[80] One question regarding polyelectrolyte adhesion that still remains unanswered is regarding adhesion involving spherical geometries. In this chapter, we have extended the electro-adhesion technique to beads and capsules. Our work shows that strong adhesion is possible between gels and beads, as well as between beads and beads. This would be advantageous for applications that require fabrication of complex geometries, sorting of different soft cargos, and their pick-up and drop-off. We have also demonstrated adhesion in completely electrostatically crosslinked beads. Our technique to adhere gels

and beads is specific to charge-polarity pair, i.e. the adhesion is possible only between oppositely charged species and that too in a very specific configuration of electric field. The process is completely reversible and is very rapid. Moreover, the technique works under water as well. We hope that the adhesion and detachment of gels and beads would be quite useful in the applications involving structurally complex tissue engineering, bio-mimicking, and adhesive drug delivery patches.

5.2 Experimental Section

Materials and Chemicals. The monomer acrylamide (Aam), the crosslinker N,N'-methylene bis(acrylamide) (BIS), the initiator ammonium persulfate (APS), the accelerant N,N,N′,N′-tetramethylethylenediamine (TEMED), the biopolymers alginate (medium molecular weight, viscosity >= 2000 cP, 2%) and chitosan (medium molecular weight, 190–310K; degree of deacetylation ~ 80%), and the reagents calcium chloride dihydrate, sodium tripolyphosphate (TPP) and glutaraldehyde solution (grade I - 50% in water) were obtained from Sigma-Aldrich. The monomer quaternized dimethylaminoethyl methacrylate (QDMAEMA) was purchased from MPD Chemicals. Magnetic γ-Fe_2O_3 nanoparticles (average surface area ≈ 42 m^2/g) were purchased from Alfa Aesar. Sodium dodecylbenzenesulfonate (SDBS) was purchased from TCI America. Graphite pencil electrode (pentel super hipolymer lead, 9mm) was purchased from Staples. The malchite green dye was from Pfaltz and Bauer, the rhodamine B dye and the methylene blue dye were purchased from Sigma-Aldrich and acid red 52 dye was obtained from TCI America. All chemicals were used as received.

Gel Preparation. All gels were made using DI water through which nitrogen gas was bubbled for 30 min to remove dissolved oxygen. 1 M Aam along with 0.24 M QDMAEMA was dissolved in DI water. Crosslinker BIS was then dissolved in the solution at the molar ratio of 1:50 w.r.t Aam. Initiator (APS) and accelerant (TEMED) were then added to the solution at concentrations of 2 mg/ml and 1.5 μL/ml, respectively. The solution was kept undisturbed in a glass petridish at room temperature in a nitrogen environment for 4 h to convert into a gel. Any unreacted monomer was washed away and gels were cut into squares of size 12 mm × 12 mm (thickness: 4 mm).

Bead / Capsule Synthesis. Beads and capsules were synthesized in a similar manner as described in chapter 4. Note that, we refer a spherical structure as a bead when it is cross-linked all the way through to the core, and refer it as a capsule when it has core-shell structure with liquid core. Droplets of 2 wt% alginate solution (containing malachite green dye) were slowly dropped into a stirring solution of 3 wt% $CaCl_2$ solution using transfer pipette and incubated for 15 min. Ca^{2+}-alginate beads were then washed and stored in DI water. The diameter of these beads was approximately 4 mm. For magnetic beads, 2 wt% γ-Fe_2O_3 was mixed with alginate before it was added dropwise into $CaCl_2$ solution. Similarly, for the chitosan-SDBS capsules, 2 wt% chitosan (in 0.2 M acetic acid) was added dropwise in 5 wt% SDBS solution. After incubating for 15 min, the capsules (diameter ~ 3 mm) were washed and stored in DI water. Chitosan-glutaraldehyde beads were formed by dropwise addition of 2 wt% chitosan into a solution of 1 wt% TPP and 2 wt% glutaraldehyde. TPP stabilizes the chitosan chains into spherical beads through electrostatic interactions followed by chemical crosslinking with glutaraldehyde.

Adhesion Strength Test. Samples for adhesion test were prepared by sandwiching 12 mm × 12 mm × 4 mm square gel and 4 mm diameter bead in between flat graphite sheets and applying the desired bias. Adhesion strength between the gel and the bead was tested using Rheometrics AR2000 stress controlled rheometer (TA instruments). The adhered gel-bead assembly was placed on the base plate with bead facing the moving plate. Constant shear rate of 0.01 s^{-1} was applied and corresponding shear stress was measured. The value of shear stress at which the bead is detached from the gel is a measure of the adhesion strength. Tests were performed using 20 mm steel plate at 25°C.

5.3 Results and Discussion

5.3.1 Adhesion and De-adhesion under Electric Field

Figure 5.1 shows adhesion of positively charged gel with a negatively charged bead. The gel is made by co-polymerization of Aam and QDMAEMA in the presence of chemical crosslinker BIS. QDMAEMA is the quaternized dimethylaminoethyl methacrylate where the nitrogen atom has a permanent positive charge. The chains of polymerized Aam and QDMAEMA are crosslinked and polymerized together to give the gel a net positive charge (schematics in Figure 5.1). The pink color of the gel is due to the presence of rhodamine B dye. When the gel is attached to a positive terminal of a power source, whose negative terminal is attached to a negatively charged calcium-alginate bead (dyed with malachite green), there is an adhesion between the two soft structures. No adhesion is observed when the polarity is reversed, i.e. positive charged gel is connected to the negative terminal and negatively charged bead is connected to the positive terminal of the power source.

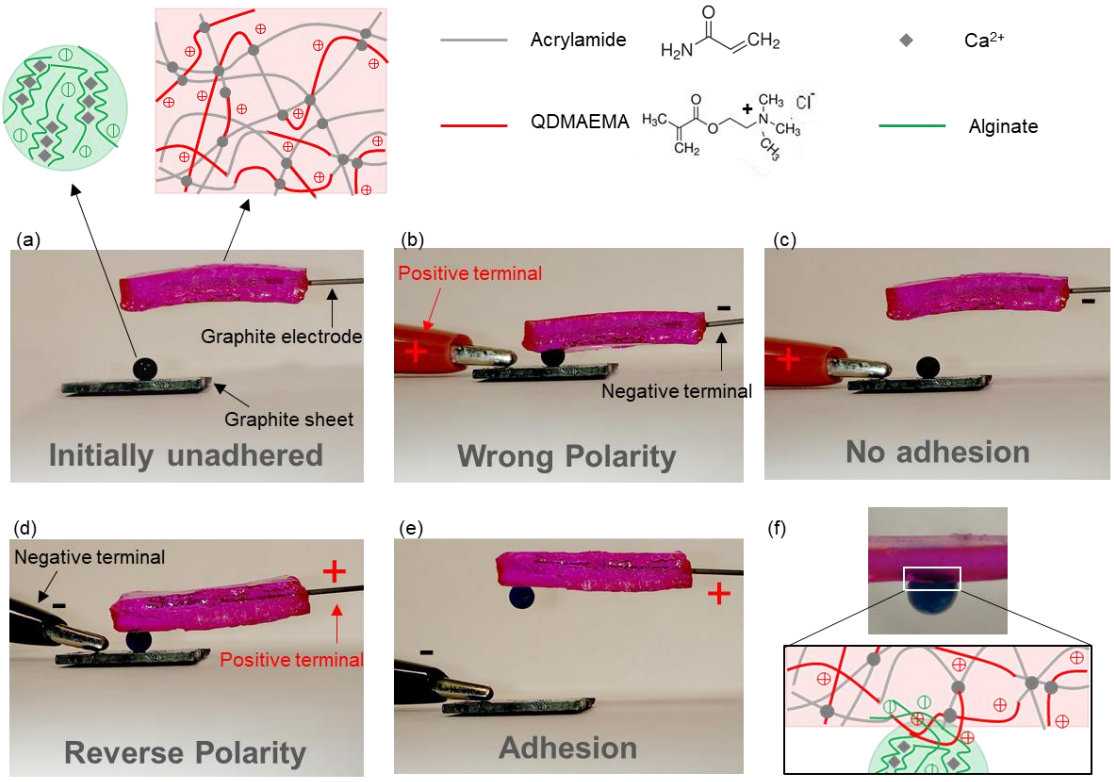

Figure 5.1. Adhesion of positively charged gel and negatively charged bead. (a) Initially gel and bead (diameter: 4 mm) were unadhered. The gel is a copolymer of uncharged monomer Aam and charged monomer QDMAEMA. The bead is a physically crosslinked network of calcium alginate where calcium ions link alginate chains through "egg-box" like junctions. (b, c) When the negatively charged bead on anode is brought in contact with positively charged gel touching cathode, no adhesion is observed. (d, e) When the polarity is reversed i.e. negatively charged bead on cathode in contact with positively charged gel on anode, there is adhesion. (f) The adhesion is attributed to electrophoretic migration of positively charged polyelectrolyte towards cathode and negatively charged polyelectrolyte towards anode. The oppositely charged chains come in contact, interpenetrate and form polyion complexes that leads to adhesion. Bias applied :10 V.

Note that the adhesion is very rapid. The images in Figure 5.1 corresponds to the case when the bias of 10 V is applied for only 5 s. The reason for the quick adhesion is believed to be the migration and interpenetration of oppositely charged chains to form

polyion complexes.[75,76] The positively charged chains in the gel feel an attraction towards the cathode and the residual negative charge on alginate chains (after crosslinking with Ca^{2+}) feel an attraction towards anode. The electrophoretic migration of chains under electric field causes the two charges to come together and form polyion complexes as shown in the last panel in Figure 5.1. No adhesion is observed upon reverse polarity because the chains would be moving in the opposite direction and would not come in contact.

Once the gel and the bead are adhered, applying a reverse polarity to the assembly i.e. positively charged gel in contact with cathode and negatively charged bead in contact with anode, causes them to detach. This is illustrated in Figure 5.2 where a bias of 10 V is applied for 10 s. It should be noted that it takes a little longer for the gel and the bead to detach in comparison to the time it took for them to attach. Again, the electrophoretic migration theory explains this behavior. The residual charges on the chains feel the electric force in the opposite direction and migrate towards the respective electrode, thereby breaking the weak polyion complexes and resulting in the detachment. The disruption of these weak bonds explains the longer detachment time (in comparison to attachment). Moreover, as shown in the top photos in Figure 5.2, no detachment of adhered assembly is observed when the polarity is such that the anode touches the positive charged gel and cathode touches the negatively charged bead.

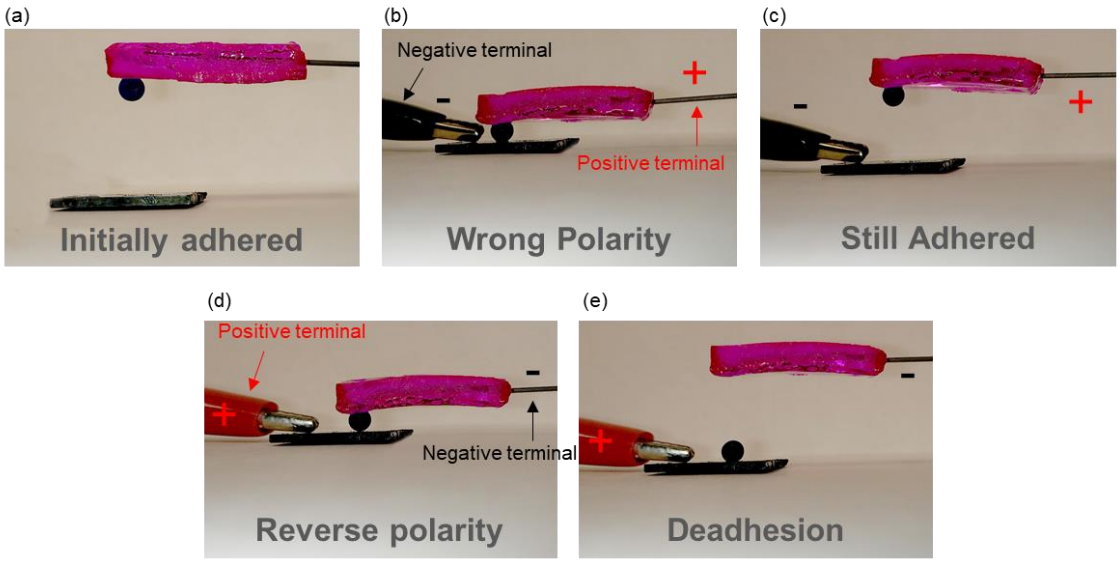

Figure 5.2. De-adhesion of positively charged gel and negatively charged bead. (a) Initially the gel and the bead (diameter: 4 mm) are adhered. (b, c) When a power source is attached to the gel-bead assembly such that the negative terminal is in contact with negatively charged bead and positive terminal to the positively charged gel, there is no detachment. (d, e) When the polarity is reversed i.e. positive terminal in contact with bead and negative terminal in contact with gel, the gel and bead detach. Bias applied: 10 V.

Several additional points regarding the adhesion and de-adhesion are worth discussing. First, the phenomenon is not restricted to a positively charged gel and a negatively charged bead. The reverse configuration works as well. We have successfully tested this behavior with a negatively charged gel (copolymer of Aam and sodium acrylate) and a positively charged capsule (chitosan-SDBS). However, the adhesion was not as strong in this case. The most likely reason for the weak adhesion is that the capsule surface is covered with SDBS, which may inhibit chitosan migration. Next, the adhesion and deadhesion is observed with different types of gels (Figure 5.3). Type 1: charged groups chemically crosslinked within the gel (Figure 5.3 - left), and type 2: charged polymer entangled within the network without any crosslinks (Figure 5.3 - right). An example of

type 1 gel is QDMAEMA gel that is chemically crosslinked with Aam. For type 2 gel, the biopolymers alginate or chitosan are mixed with the Aam monomer before gelation and therefore, their chains are entangled inside the network without any crosslinks. Both types of gels show adhesion and detachment in the presence of electric field. This has been observed in the literature as well with gel-gel adhesion.[81] It should also be noted that the adhesion and detachment occurs under water as well (discussed later) and the electrodes do not need to be in contact with the gel or the capsule. However, the non-contact adhesion is weak and takes a longer time. Therefore, all the further experiments were conducted with electrodes touching the materials.

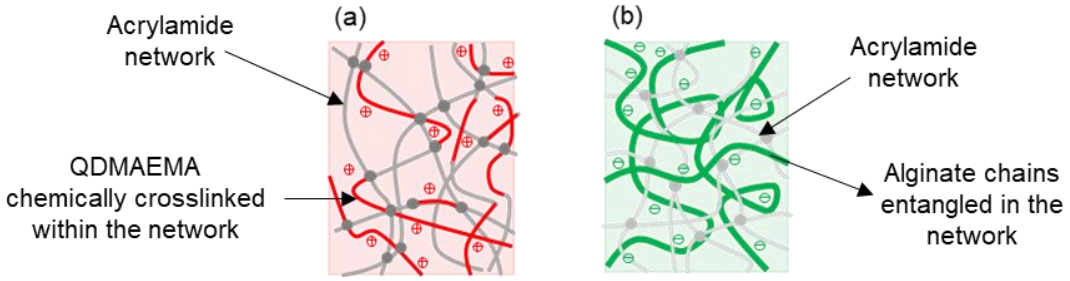

Figure 5.3. Schematics showing two types of gels. (a) Charged monomer is chemically crosslinked with uncharged monomer into a network to form the gel. Red coloured chain segments represent charged monomer. (b) Charged polymer chains are entangled into the network of uncharged gel. There are no crosslinks between the charged and uncharged groups.

5.3.2 Bead - Capsule Adhesion

Electric field induced adhesion discussed in the previous section is not restricted to gel and bead geometry only. In this section, we demonstrate that such adhesion and detachment can be achieved with two spherical geometries as well. As long as there is contact between the oppositely charged groups and there is migration under electric field, there will be adhesion. Figure 5.4 illustrates the adhesion between Ca^{2+}-alginate bead (dyed pink with acid red 52) and chitosan-SDBS capsule (dyed blue with methylene blue). A bias of 10 V is applied for 10 s with cathode in contact with alginate bead and anode in contact with chitosan capsule. On reversing the polarity, they detach.

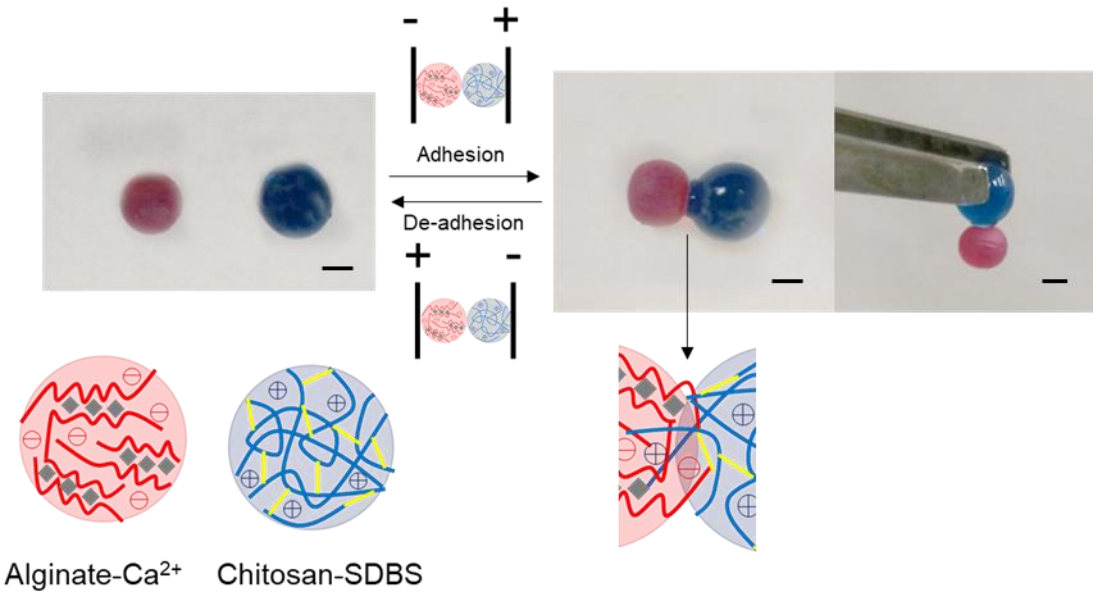

Figure 5.4. Bead - Capsule Adhesion. Electrically induced adhesion between negatively charged calcium-alginate bead (red) and positively charged chitosan-SDBS capsule (blue). For adhesion, negative terminal is connected to calcium-alginate bead and positive terminal is connected to chitosan-SDBS capsule. Schematics show the interpenetration and electrostatic bonding of oppositely charged chains after electrophoretic migration. Reversing the polarity causes detachment. Bias applied: 10 V, scale bar: 2 mm.

5.3.3 Adhesion Strength

The adhesion between the gel and the capsule discussed in Section 5.5.1 is quite robust. It is not attained by simple pressure bonding without electrical signal. To demonstrate extent of the adhesive strength, we synthesized Ca^{2+}- alginate beads with Fe_2O_3 magnetic nanoparticles. These magnetic alginate beads can be easily manipulated and propelled using a neodymium magnet.

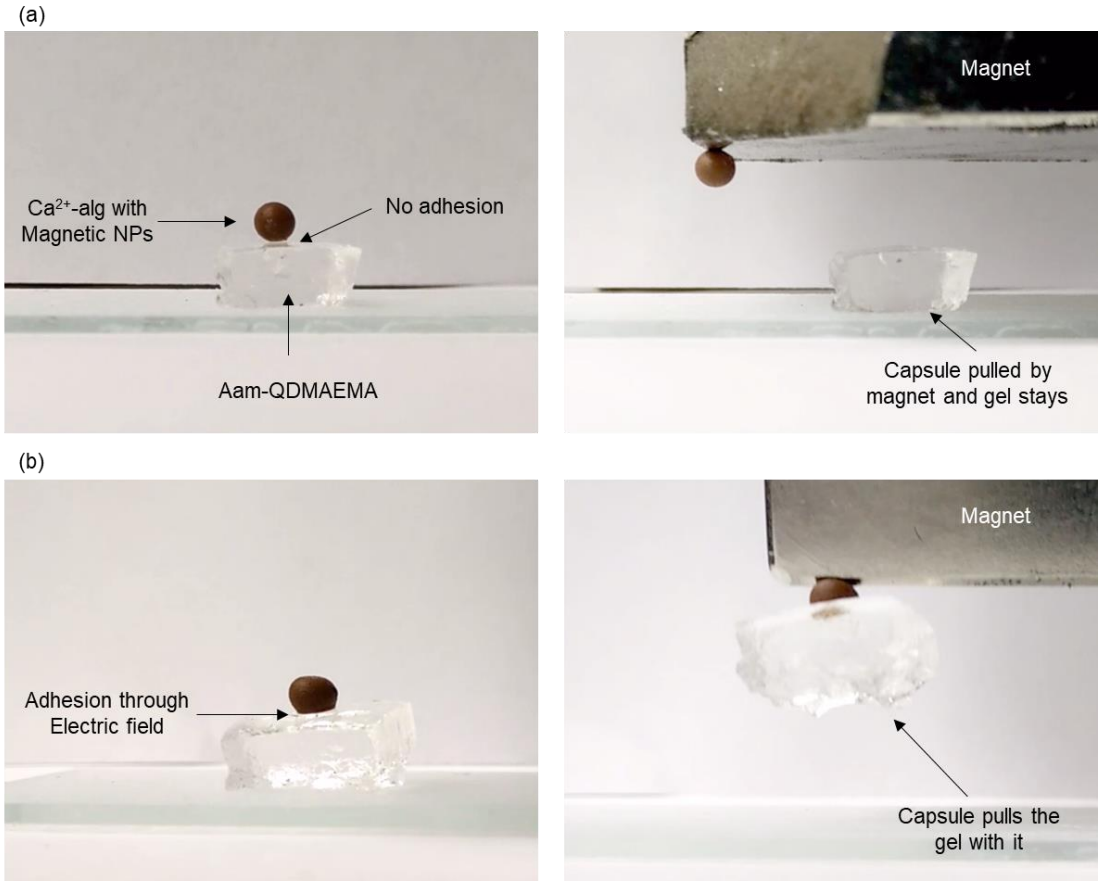

Figure 5.5. Adhesion between magnetic alginate bead and QDMAEMA gel. (a) No adhesion between gel and bead without electric field. When a neodymium magnet is brought close to the assembly, the bead gets attached to the magnet whereas the gel stays put. (b) When an electrical bias of 10 V is applied for 10 s, a strong adhesion develops between the gel and the bead. Now, upon bringing a magnet, the whole assembly gets attached to the magnet, indicating a strong adhesion between the gel and the bead.

We compared the adhesion between the magnetic alginate bead and QDMAEMA gel attained with and without electrical bias by bringing a magnet near the adhered structure. Top panels in Figure 5.5 shows that when the gel and the bead is simply pressure bonded (pressed against each other for 10 s) no significant adhesion is achieved. When a neodymium magnet is brought next to the assembly, the bead moves and attaches to the magnet. However, when the bead and the gel are adhered using electric field (10 V, 10 s), the adhesion is strong. Now, upon bringing the magnet near the adhered structure, the magnetic bead pulls the gel along with it as it attaches to the magnet, indicating a strong adhesion between the bead and the gel (bottom panels in Figure 5.5).

Next, we quantified the strength of adhesion between the Ca^{2+}-alginate bead and the Aam-QDMAEMA gel. Figure 5.6a shows the image of the setup to adhere the gel and the bead. As described in the experimental section, we placed the adhered gel-bead assembly on a rheometer and applied a constant shear rate of 0.01 s^{-1} (Figure 5.6b). The shear stress required to maintain the shear rate is recorded over time. The value of shear stress goes up until the bead gets detached off the gel and then the value drops. The highest value of shear stress just before the bead is snapped off is used as the measure of adhesion strength.

Figure 5.7 depicts the strength of adhesion as a function of adhesion time. A bias of 10 V is applied for different times and shear stress on the adhered structure is measured. The longer time the electric field is applied, the stronger the adhesion is. This can be explained by the fact that the longer adhesion time allows larger electrophoretic migration of chains and thus form stronger electrostatic complexes resulting in increased strength.

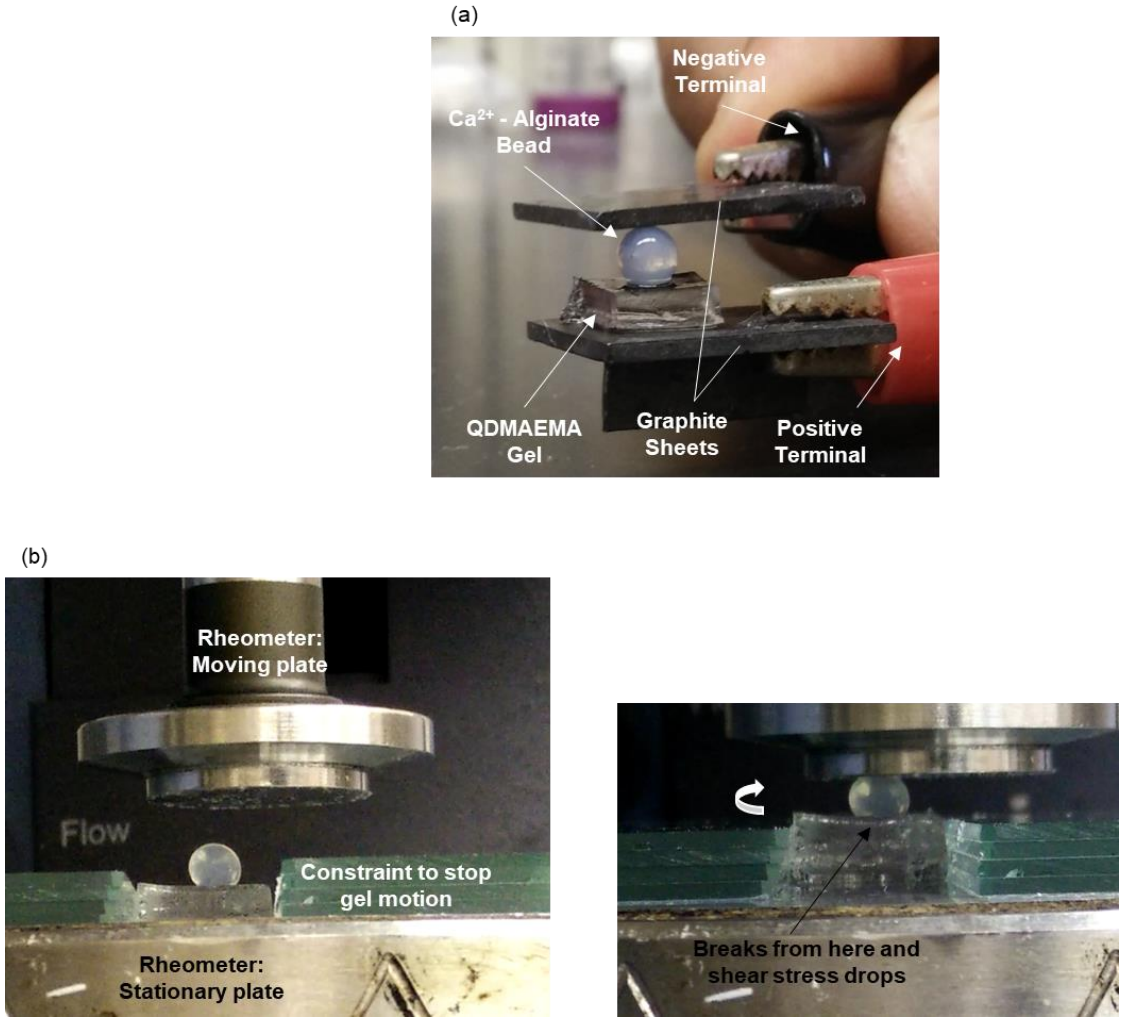

Figure 5.6. Strength of adhesion. (a) Adhesion between the gel and the bead is achieved by attaching negative electrode to the bead and positive electrode to the gel. (b) Measuring strength of adhesion using a rheometer. The gel-bead adhered assembly is put on a stationary plate of the rheometer. 20 mm steel plate geometry is used to apply constant shear rate of 0.01 s^{-1}. The shear stress required to maintain this shear rate is recorded. Once the bead gets detached from the gel, the shear stress drops. The value of shear stress just before the bead detaches is conceived as the measure of adhesion strength.

The strength of adhesion w.r.t. applied voltage is quantified in Figure 5.8. The adhesion time is kept constant at 10 s. Again, the larger voltage would allow larger

migration of charged polyelectrolytes and better polyion complexes and therefore would create stronger adhesion. Hence, the adhesion strength goes up with applied voltage. Note the differences in the way the adhesion strength goes up w.r.t. the adhesion time (Figure 5.7) and w.r.t. the voltage (Figure 5.8). There is monotonous increase in the adhesion strength with both variables. However, with adhesion time, the strength plateaus unlike with the voltage. When varying the adhesion time, we kept the applied voltage constant at 10 V. Therefore, the electric force that the charged polyion chains experience is constant. As they start migration they feel resistance from the other end. Although, the adhesion strength goes up over time, the resistance these chains feel against migration also goes up. At some point during the process, the forces balance, ceasing any further migration and therefore the adhesion strength plateaus. On the contrary, when the applied voltage is increased, the force experienced by the chains increases proportionally, and therefore the strength of adhesion increases without any plateauing.

Next, we studied the effect of the amount of charged groups on the adhesion strength. Since the charge on the gel is due to the presence of charged monomer QDMAEMA, by changing the moles of QDMAEMA, we changed the effective charge on the gel. Figure 5.9 shows the effect of QDMAEMA concentration on the adhesion strength. As the charge on the gel goes up, the effective number of polyion complexes formed after migration under electric field, would go up as well. The increase in interaction between oppositely charged groups increases the adhesive strength as shown in Figure 5.9.

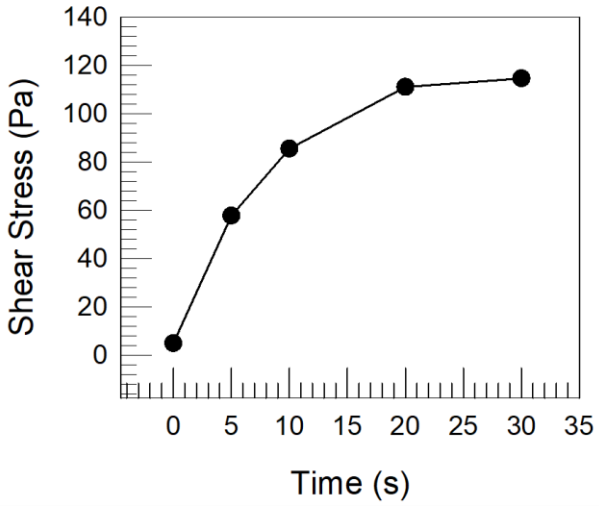

Figure 5.7. Strength of adhesion w.r.t. adhesion time. As the adhesion time goes up, the polyelectrolyte chains in the gel and the bead can migrate for longer time and form more polyion complexes. This is expressed as increase in adhesion strength. Finite value of shear stress at 0 s corresponds to the stress required to roll of the unadhered bead on the gel surface. All tests were performed at 10 V bias.

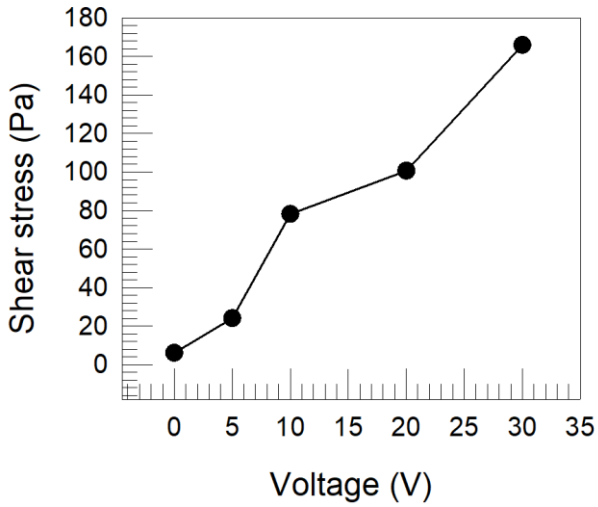

Figure 5.8. Strength of adhesion w.r.t. applied voltage. Higher voltage between the terminals would exert stronger force on the polyelectrolyte chains in the gel and the bead, forcing them to migrate more and form more polyion complexes. As a result, the shear stress increases with increasing voltage. All tests were performed for 10 s adhesion time.

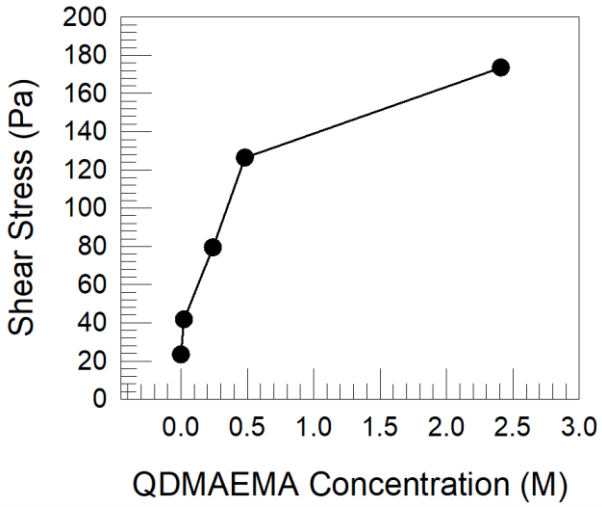

Figure 5.9. Strength of adhesion w.r.t. charged monomer content (QDMAEMA). The electro-adhesion is attributed to the electrophoretic migration of chains and formation of weak electrostatic bonds between the charged groups. Larger amount of charge would result in more bonds and therefore increase in adhesion strength. More shear stress would be required to disrupt these bonds as reflected the plot by the increase in shear stress with increasing charged content. All tests were performed for at 10 V bias for 10 s.

5.3.4 Pick-up and Transfer Controlled by Electric Field Polarity

The instantaneous adhesion and detachment between the oppositely charged gel and bead has many applications. One such application is shown in Figure 5.10. Three beads are transferred one by one from surface 1 to surface 2 using oppositely charged gel. In this case, surface 1 is connected to the negative terminal of a power source. The positively charged QDMAEMA gel is connected to the positive terminal through a graphite electrode. When a bias of 10 V is applied and the gel is brought in contact with Ca^{2+}-alginate bead on surface 1, they are instantaneously adhered as shown in Figure 5.10. Thereafter, we changed the polarity of the electrode connected to the gel from positive to negative. Surface 2 is connected to the positive terminal. When the gel-bead adhered assembly is brought in

contact with surface 2, there is an instantaneous detachment and the bead is placed on surface 2. This way by adjusting electrical polarity, the bead is picked up from surface 1 and transferred to surface 2. Note that the pick-up and drop-off does not occur with the reverse polarities, i.e. if the negative terminal connected to the gel is contacted with the bead on the positive terminal connected surface 1, no adhesion is observed. Similarly, when the positive terminal connected to the gel-bead assembly is contacted to the negative terminal connected surface 2, no detachment is observed. Moreover, same charged gel and bead do not adhere irrespective of the polarity. This demonstrates that the technique to adhere and detach is very specific to charge-polarity pair and can be utilized for soft cargo transport.

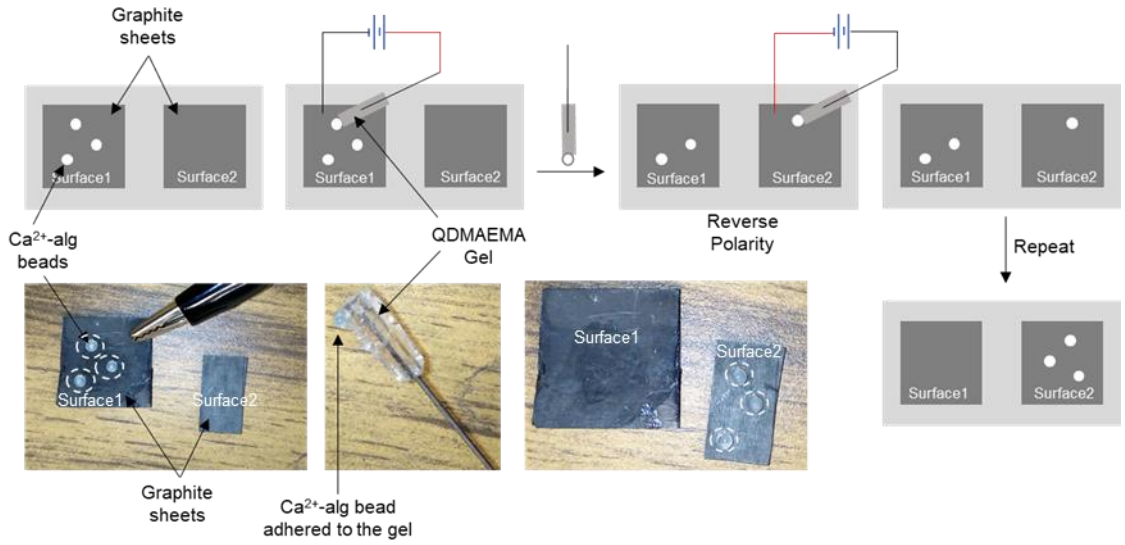

Figure 5.10. Pick-up and transfer controlled by electric-field Polarity. Pick-up and drop-off of negatively charged Ca^{2+}-alg bead from one surface to another using QDMAEMA gel. Beads can be picked up when the polarity is such that negatively charged bead is at negative terminal and positively charged gel is at positive terminal. Drop off is achieved when polarity is reversed. Three beads are transferred one by one from surface 1 to surface 2.

5.3.5 Under Water Sorting of Beads

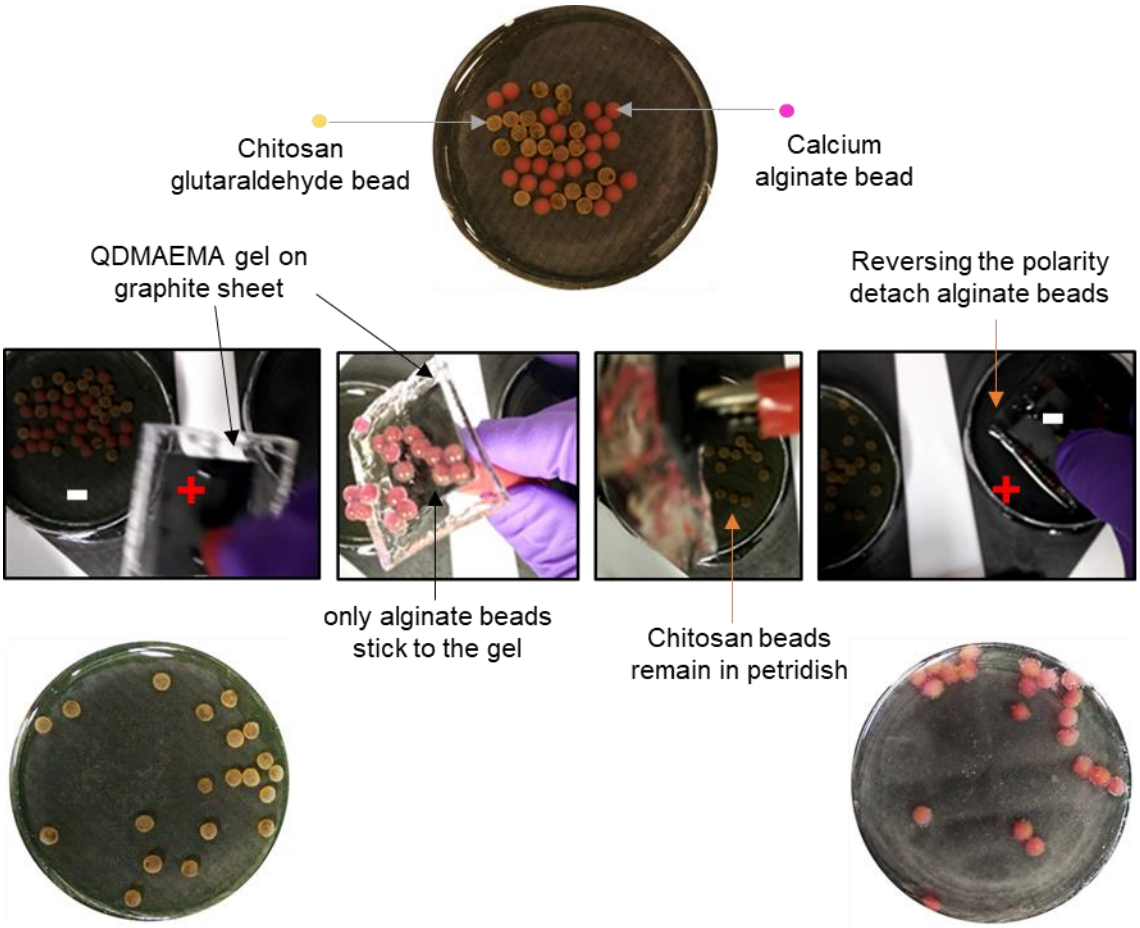

Figure 5.11. Sorting of beads under water. Two types of beads are mixed and sorted using the adhesion-detachment technique. Mixture of calcium-alginate beads (red) and chitosan-glutaraldehyde beads (yellow) is placed under water on the conducting graphite plate. When the positively charged gel is brought next to the mixture and a bias of 10V is applied, only the pink beads get adhered to the gel. Yellow beads remain inert in the petridish. The adhered pink beads are transferred to another petridish by reversing the polarity that leads to detachment. Initial mixture of beads is sorted and separated into two groups of similar beads.

As mentioned earlier, the adhesion and de-adhesion of soft gel and bead is not limited to open air environment. The behavior is observed under water as well. This is illustrated in Figure 5.11 where we demonstrate sorting of beads under water. Two kinds of beads (a) Ca^{2+}-alginate (pink) and (b) chitosan-glutaraldehyde (yellow) are mixed and

placed in a petridish, which is modified to have a flat graphite base as shown in the top image in Figure 5.11. The graphite base is connected to the negative terminal of a power source, whose positive terminal is connected to another graphite sheet that is attached to a large square piece of QDMAEMA gel. When a bias of 10 V is applied and the gel is brought in contact with the beads, only the negatively charged Ca^{2+}-alginate beads are attached to the gel. Chitosan-glutaraldehyde beads remain in the petridish. The Ca^{2+}-alginate beads are then transferred to another petridish by reversing the polarity. Images in Figure 5.11 demonstrate the sorting of two kinds of beads from their mixture.

5.4 Conclusions

We have described an electro-adhesion technique where oppositely charged gels and beads (or capsules) can be reversibly attached/detached instantaneously. The adhesion and detachment is dependent on charge-polarity pair, i.e. only oppositely charged gel-bead system would adhere and that too in a certain polarity configuration. Anionic polymer in contact with cathode and cationic polymer in contact with anode leads to adhesion and reverse polarity leads to detachment. The technique works for purely physically crosslinked polymers, purely chemically crosslinked polymers, as well as their combinations. Adhesion and detachment also works under water and without the direct contact with the electrodes. We have illustrated two applications of the technique: (1) pick-up and drop-off of the beads from one surface to another; (2) sorting of two types of beads from their mixture. One remarkable feature of the process is that it is very rapid and occurs within a few seconds. This would be advantageous for applications that require fast response times.

Chapter 6

Conclusions and Recommendations

6.1 Project Summary and Principal Contributions

In this dissertation, we have shown three different ways an electrical stimulus can interact with soft matter. All of the three studies were conducted at relatively low voltage and current values, achieving significant effects at biologically safe conditions. Manipulating the ways electric field can interact with charged species in solution and in air, we have achieved (1) gelation of biopolymers, (2) disruption of charged beads and capsules, and (3) reversible adhesion between oppositely charged gels and beads.

In Chapter 3, we have described a gelation technique to form hollow biopolymer gel structures that are difficult to make using traditional methods. This was achieved by entrapping crosslinking cations in a thermo-responsive polymer gel. Use of the thermo-responsive polymer provides dual advantages: (1) mold in the suitable shape can be designed to get the final gel in desired geometry; (2) thermo-responsiveness allows the mold to be melted away to get the final gel. When a potential bias is applied across the mold and the bio-polymer solution, the cross-linking ions migrate out of the mold and gel the biopolymer. No significant diffusion of ions in the absence of electrical stimulus, provides an excellent “on-off” switch to trigger gelation on demand. Multilayer structures with capabilities to immobilize biological species make this technique exciting. Moreover, with the use of commercially available hydrophobic coating, patterned gel can be developed.

In Chapter 4, we reported a unique behavior of biopolymer beads and capsules under DC electric field. Negatively charged Cu^{2+}-alginate beads undergo swelling and breaking from the side closer to the anode. The anisotropy in the response might be the result of anisotropic distribution of mobile ions that take place when a polyelectrolyte gel is placed under electric field. The beads were synthesized through simple dropwise addition of biopolymer solution into oppositely charged medium. These beads can be triggered by electrical stimulus remotely, i.e. the beads do not have to be in direct contact with the electrodes. The swelling and breaking behavior of the beads have been observed at both macro and micro scale. We have demonstrated an electro-actuated valving application utilizing the response of the beads.

In Chapter 5, we demonstrated electrically induced reversible adhesion between oppositely charged gel and bead. The adhesion is specific to charge-polarity pair, i.e. adhesion occurs only when positively charged species is next to anode and negatively charged species is next to the cathode. Reversing the polarity causes de-adhesion in already adhered system. The adhesion and detachment is a result of electrophoretic migration of oppositely charged polyelectrolytes under electric field. During adhesion, the polyelectrolyte chains interpenetrate and form polyion complexes. On reversing the polarity, the complexes dissociate and charged polymeric chains move in opposite directions that leads to detachment. We have quantified the strength of adhesion by measuring the shear stress required to split the gel and the bead. Additionally, we have applied the technique to pick-up and drop-off soft cargo and to demonstrate under water sorting of different beads from their mixture.

6.2 Recommendations for Future Work

6.2.1 Multicompartment Capsules

Containers with separated inner compartments that can perform simultaneous or cascade reactions, while keeping encapsulated reactants separated (from the products that is freely diffusing in the same environment), are extremely attractive for applications of catalysis,[82-84] drug delivery,[85,86] and tissue engineering.[87,88] Such multicompartment containers on the micron scale are considered artificial cells, due to the overall structure being similar to organelles enclosed in discrete, functional membranes within the cell. Our lab has recently shown bacterial signaling using multicompartment capsules.[44] We propose to combine the electro-induced breaking of capsules discussed in Chapter 4 with the multi-compartment capsule for release applications. We can incorporate multiple functionalities in the multicompartment capsule by selectively making certain capsules electro responsive. For example, we can make the outer container rupture under electric field and release the inner containers that are inert. In contrast, we can also make the outer compartment inert and make some of the inner compartment electro responsive and some inert. Upon applying the electrical stimulus, we can break some of the inner compartment and release encapsulated chemical species that can trigger cascade reactions with electrically inert inner compartment, all the while safely encapsulated in the inert outer compartment.

Figure 6.1 shows the preliminary result of electro-responsive capsules in multicompartment setting at macro scale. The schematics show the procedure used to make the multicompartment capsules. The outer compartment is chitosan-SDBS, which is shown to be electro responsive (as discussed in Chapter 4). The inner compartments are made by

chemically crosslinking chitosan with glutaraldehyde. The chemically crosslinked beads are too rigid to undergo any volume transformation and thus are electrically inert. When the electrical stimulus is applied, the outer chitosan-SDBS compartment breaks while the inner compartment remains inert as shown in Figure 6.1.

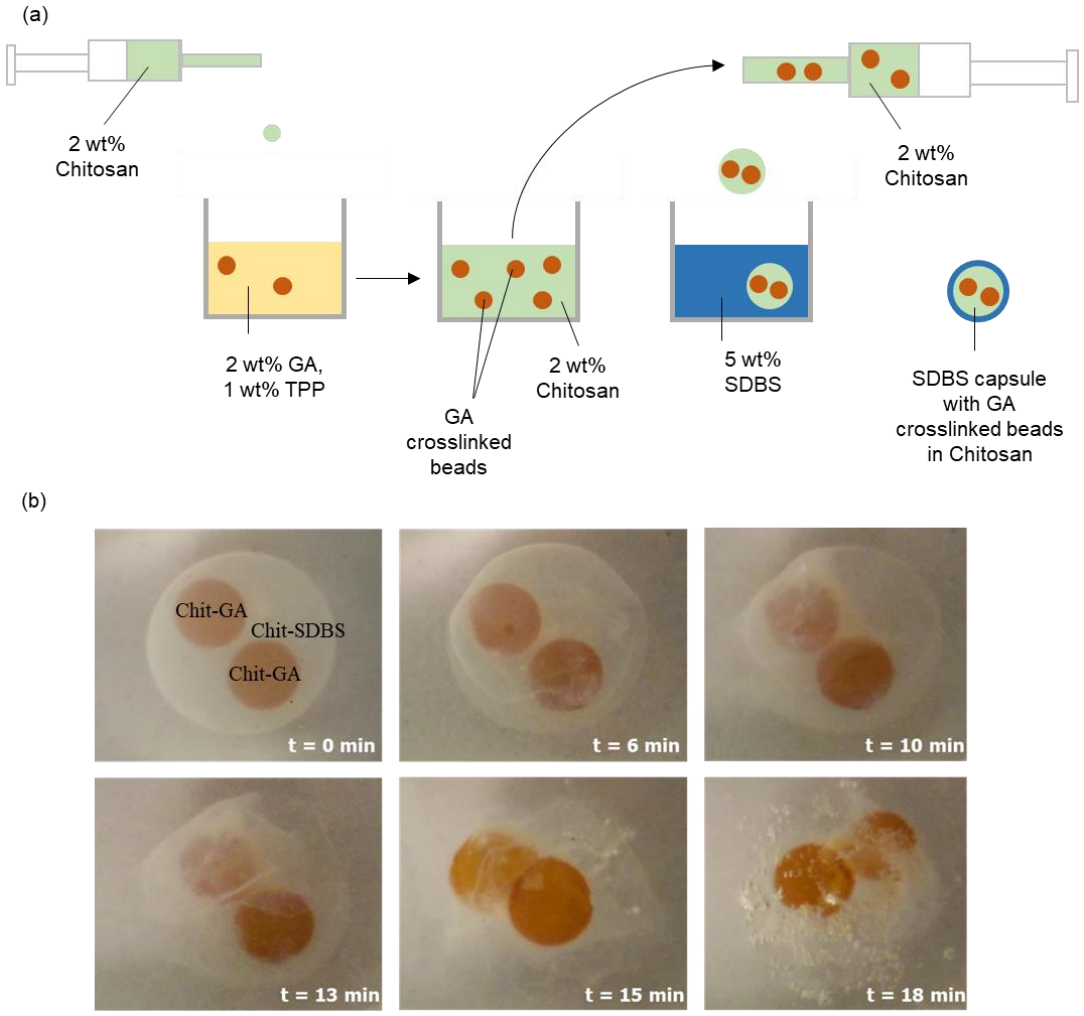

Figure 6.1. Multicompartment electro-responsive capsules. (a) Schematics describing the procedure to make multicompartment capsule. Chitosan is dropped in glutaraldehyde (GA) and sodium tripolyphosphate (TPP) solution to form inert beads. These beads are suspended in fresh chitosan, which was then dropped into SDBS solution to form multicompartment capsule. (b) Electro-response of multicompartment capsule where the outer chitosan-SDBS capsule breaks under electrical stimulus releasing inner unaffected chitosan-GA beads.

6.2.2 Electro-induced Adhesion at Microscale

Micromanipulation is a technique where delicate manipulations of a specimen are performed under a microscope. This is particularly important in the fields of single cell adhesion studies,[89] in vitro fertilization (IVF), and electrophysiology.[90] An exciting future research would be to study our electro-induced reversible adhesion at small scales. If we could selectively pick and drop microparticles through adhesion and detachment, it would be beneficial for micromanipulation community. Moreover, since the technique works under water as well, reversible micro-adhesion would be important for manipulation of biological samples that are inherently aqueous based.

Microscale adhesion can be significantly different from the macro adhesion presented in Chapter 5.[91,92] Due to large surface area to volume ratio at small scales, many microparticles can be inherently adhesive. This may be a problem if we want to achieve selective adhesion through directional electric field. Therefore, additional studies are warranted regarding adhesive forces at micro-scale before our electro-induced adhesion can be extended at such scale. Further study in this regard would make for an exciting future work.

References

[1] Tanaka, T. "Gels." *Scientific American* **1981**, *244*, 124-138.

[2] Osada, Y.; Ping Gong, J.; Tanaka, Y. "Polymer Gels." *Journal of Macromolecular Science, Part C* **2004**, *44*, 87-112.

[3] Oh, H. "Photoresponsive Systems Based on Self-Assembly". Ph.D. Dissertation, University of Maryland, 2014.

[4] Athas, J. C.; Nguyen, C. P.; Zarket, B. C.; Gargava, A.; Nie, Z.; Raghavan, S. R. "Enzyme-Triggered Folding of Hydrogels: Toward a Mimic of the Venus Flytrap." *ACS applied materials & interfaces* **2016**, *8*, 19066-19074.

[5] Morales, D.; Palleau, E.; Dickey, M. D.; Velev, O. D. "Electro-actuated hydrogel walkers with dual responsive legs." *Soft Matter* **2014**, *10*, 1337-1348.

[6] Kwon, G. H.; Park, J. Y.; Kim, J. Y.; Frisk, M. L.; Beebe, D. J.; Lee, S.-H. "Biomimetic Soft Multifunctional Miniature Aquabots." *Small* **2008**, *4*, 2148-2153.

[7] Wadhwa, R.; Lagenaur, C. F.; Cui, X. T. "Electrochemically controlled release of dexamethasone from conducting polymer polypyrrole coated electrode." *Journal of Controlled Release* **2006**, *110*, 531-541.

[8] Lim, H. L.; Chuang, J. C.; Tran, T.; Aung, A.; Arya, G.; Varghese, S. "Dynamic Electromechanical Hydrogel Matrices for Stem Cell Culture." *Advanced Functional Materials* **2011**, *21*, 55-63.

[9] Markx, G. H. "The use of electric fields in tissue engineering: A review." *Organogenesis* **2008**, *4*, 11-17.

[10] TANAKA, T.; NISHIO, I.; SUN, S.-T.; UENO-NISHIO, S. "Collapse of Gels in an Electric Field." *Science* **1982**, *218*, 467-469.

[11] Discher, D. E.; Janmey, P.; Wang, Y.-l. "Tissue cells feel and respond to the stiffness of their substrate." *Science* **2005**, *310*, 1139-1143.

[12] Shiladitya, B.; Marchetti, M. C. "Controlling cell–matrix traction forces by extracellular geometry." *New Journal of Physics* **2013**, *15*, 035015.

[13] Liechty, W. B.; Kryscio, D. R.; Slaughter, B. V.; Peppas, N. A. "Polymers for Drug Delivery Systems." *Annual review of chemical and biomolecular engineering* **2010**, *1*, 149-173.

[14] Lee, K. Y.; Mooney, D. J. "Alginate: properties and biomedical applications." *Progress in polymer science* **2012**, *37*, 106-126.

[15] Pawar, S. N.; Edgar, K. J. "Alginate derivatization: A review of chemistry, properties and applications." *Biomaterials* **2012**, *33*, 3279-3305.

[16] Augst, A. D.; Kong, H. J.; Mooney, D. J. "Alginate Hydrogels as Biomaterials." *Macromolecular Bioscience* **2006**, *6*, 623-633.

[17] Haug, A. "The effect of divalent metals on the properties of alginate solutions." *Acta Chem. Scand* **1965**, *19*, 341-351.

[18] Haug, A.ŧAffinity of some divalent metals to different types of alginates.ŧ **1961**, *15*, 1794-&.

[19] Ravi Kumar, M. N. V. "A review of chitin and chitosan applications." *Reactive and Functional Polymers* **2000**, *46*, 1-27.

[20] Rinaudo, M. "Chitin and chitosan: Properties and applications." *Progress in Polymer Science* **2006**, *31*, 603-632.

[21] Bhattarai, N.; Gunn, J.; Zhang, M. "Chitosan-based hydrogels for controlled, localized drug delivery." *Advanced Drug Delivery Reviews* **2010**, *62*, 83-99.

[22] Macquarrie, D. J.; Bacheva, A. "Efficient subtilisin immobilization in chitosan, and peptide synthesis using chitosan-subtilisin biocatalytic films." *Green Chemistry* **2008**, *10*, 692-695.

[23] Chatterjee, S.; Chatterjee, T.; Woo, S. H. "A new type of chitosan hydrogel sorbent generated by anionic surfactant gelation." *Bioresour Technol* **2010**, *101*, 3853-8.

[24] Srinatha, A.; Pandit, J. K.; Singh, S. "Ionic Cross-linked Chitosan Beads for Extended Release of Ciprofloxacin: In vitro Characterization." *Indian Journal of Pharmaceutical Sciences* **2008**, *70*, 16-21.

[25] Tako, M. "The principle of polysaccharide gels." *Advances in Bioscience and Biotechnology* **2015**, *6*, 22.

[26] "Bioresearch-Lonza." *can be accessed at* http://bio.lonza.com/uploads/tx_mwaxmarketingmaterial/Lonza_BenchGuides_SourceBook_Appendix_B_-_Agarose_Physical_Chemistry.pdf.

[27] Lee, P. Y.; Costumbrado, J.; Hsu, C.-Y.; Kim, Y. H. "Agarose Gel Electrophoresis for the Separation of DNA Fragments." *Journal of Visualized Experiments : JoVE* **2012**, 3923.

[28] Mercey, E.; Obeïd, P.; Glaise, D.; Calvo-Muñoz, M.-L.; Guguen-Guillouzo, C.; Fouqué, B. "The application of 3D micropatterning of agarose substrate for cell culture and in situ comet assays." *Biomaterials* **2010**, *31*, 3156-3165.

[29] Wittrup, K. D.; Verdine, G. L. *Protein Engineering for Therapeutics*; Elsevier Science, 2012.

[30] Armisen, R.; Galatas, F. "Production, properties and uses of agar." **1987**.

[31] Hirose, Y.; Giannetti, G.; Marquardt, J.; Tanaka, T. "Migration of Ions and pH Gradients in Gels under Stationary Electric Fields." *Journal of the Physical Society of Japan* **1992**, *61*, 4085-4097.

[32] Liu, Y.; Zhang, B.; Gray, K. M.; Cheng, Y.; Kim, E.; Rubloff, G. W.; Bentley, W. E.; Wang, Q.; Payne, G. F. "Electrodeposition of a weak polyelectrolyte hydrogel: remarkable effects of salt on kinetics, structure and properties." *Soft Matter* **2013**, *9*, 2703-2710.

[33] Wang, Z.; Zhang, X.; Gu, J.; Yang, H.; Nie, J.; Ma, G. "Electrodeposition of alginate/chitosan layer-by-layer composite coatings on titanium substrates." *Carbohydrate Polymers* **2014**, *103*, 38-45.

[34] MORALES, D. H. "Hydrogel Actuation by Electric Field Driven Effects". Ph.D. Dissertation, North Carolina State University, 2015.

[35] Qiu, Y.; Park, K. "Environment-sensitive hydrogels for drug delivery." *Advanced Drug Delivery Reviews* **2001**, *53*, 321-339.

[36] Esser-Kahn, A. P.; Odom, S. A.; Sottos, N. R.; White, S. R.; Moore, J. S. "Triggered Release from Polymer Capsules." *Macromolecules* **2011**, *44*, 5539-5553.

[37] Osada, Y.; Okuzaki, H.; Hori, H. "A polymer gel with electrically driven motility." *Nature* **1992**, *355*, 242-244.

[38] Shiga, T.; Hirose, Y.; Okada, A.; Kurauchi, T. "Electrically driven polymer gel finger working in the air." *Journal of intelligent material systems and structures* **1993**, *4*, 553-557.

[39] Svirskis, D.; Travas-Sejdic, J.; Rodgers, A.; Garg, S. "Electrochemically controlled drug delivery based on intrinsically conducting polymers." *Journal of Controlled Release* **2010**, *146*, 6-15.

[40] Kajiwara, K.; Ross-Murphy, S. B. "Synthetic gels on the move." *Nature* **1992**, *355*, 208-209.

[41] Irie, M. "Photoresponsive polymers. Reversible bending of rod-shaped acrylamide gels in an electric field." *Macromolecules* **1986**, *19*, 2890-2892.

[42] Zinger, B.; Miller, L. L. "Timed release of chemicals from polypyrrole films." *Journal of the American Chemical Society* **1984**, *106*, 6861-6863.

[43] Haider, S.; Park, S.-Y.; Saeed, K.; Farmer, B. L. "Swelling and electroresponsive characteristics of gelatin immobilized onto multi-walled carbon nanotubes." *Sensors and Actuators B: Chemical* **2007**, *124*, 517-528.

[44] Lu, A. X. "Microfluidic Generation of Anisotropic Capsules". Ph.D. Dissertation, University of Maryland, 2015.

[45] Ouwerx, C.; Velings, N.; Mestdagh, M. M.; Axelos, M. A. V. "Physico-chemical properties and rheology of alginate gel beads formed with various divalent cations." *Polymer Gels and Networks* **1998**, *6*, 393-408.

[46] Mørch, Ý. A.; Donati, I.; Strand, B. L. "Effect of Ca2+, Ba2+, and Sr2+ on Alginate Microbeads." *Biomacromolecules* **2006**, *7*, 1471-1480.

[47] Martinsen, A.; Skjåk-Bræk, G.; Smidsrød, O. "Alginate as immobilization material: I. Correlation between chemical and physical properties of alginate gel beads." *Biotechnology and Bioengineering* **1989**, *33*, 79-89.

[48] Osada, Y.; Kishi, R.; Hasebe, M. *Polym Sci Part C: Polym Lett* **1987**.

[49] Kishi, R.; Hasebe, M.; Hara, M.; Osada, Y. "Mechanism and process of chemomechanical contraction of polyelectrolyte gels under electric field." *Polymers for Advanced Technologies* **1990**, *1*, 19-25.

[50] Zvitov, R.; Nussinovitch, A. "Weight, mechanical and structural changes induced in alginate gel beads by DC electrical field." *Food Hydrocolloids* **2001**, *15*, 33-42.

[51] Glazer, P. J.; van Erp, M.; Embrechts, A.; Lemay, S. G.; Mendes, E. "Role of pH gradients in the actuation of electro-responsive polyelectrolyte gels." *Soft Matter* **2012**, *8*, 4421-4426.

[52] Doi, M.; Matsumoto, M.; Hirose, Y. "Deformation of ionic polymer gels by electric fields." *Macromolecules* **1992**, *25*, 5504-5511.

[53] Jin, S.; Gu, J.; Shi, Y.; Shao, K.; Yu, X.; Yue, G. "Preparation and electrical sensitive behavior of poly (N-vinylpyrrolidone-co-acrylic acid) hydrogel with flexible chain nature." *European Polymer Journal* **2013**, *49*, 1871-1880.

[54] Kwon, I. C.; Bae, Y. H.; Kim, S. W. "Characteristics of charged networks under an electric stimulus." *Journal of Polymer Science Part B: Polymer Physics* **1994**, *32*, 1085-1092.

[55] Gong, J. P.; Nitta, T.; Osada, Y. "Electrokinetic Modeling of the Contractile Phenomena of Polyelectrolyte Gels. One-Dimensional Capillary Model." *The Journal of Physical Chemistry* **1994**, *98*, 9583-9587.

[56] Shiga, T.; Hirose, Y.; Okada, A.; Kurauchi, T. "Bending of ionic polymer gel caused by swelling under sinusoidally varying electric fields." *Journal of Applied Polymer Science* **1993**, *47*, 113-119.

[57] De Rossi, D. E.; Chiarelli, P.; Buzzigoli, G.; Domenici, C.; Lazzeri, L. "Contractile behavior of electrically activated mechanochemical polymer actuators." *ASAIO transactions* **1986**, *32*, 157-162.

[58] Cipriano, B. H.; Banik, S. J.; Sharma, R.; Rumore, D.; Hwang, W.; Briber, R. M.; Raghavan, S. R. "Superabsorbent hydrogels that are robust and highly stretchable." *Macromolecules* **2014**, *47*, 4445-4452.

[59] Gargava, A.; Arya, C.; Raghavan, S. R. "Smart Hydrogel-Based Valves Inspired by the Stomata in Plants." *ACS Applied Materials & Interfaces* **2016**, *8*, 18430-18438.

[60] Laftah, W. A.; Hashim, S.; Ibrahim, A. N. "Polymer Hydrogels: A Review." *Polymer-Plastics Technology and Engineering* **2011**, *50*, 1475-1486.

[61] Gong, J. P.; Katsuyama, Y.; Kurokawa, T.; Osada, Y. "Double-Network Hydrogels with Extremely High Mechanical Strength." *Advanced Materials* **2003**, *15*, 1155-1158.

[62] Yuk, H.; Zhang, T.; Lin, S.; Parada, G. A.; Zhao, X. "Tough bonding of hydrogels to diverse non-porous surfaces." *Nat Mater* **2016**, *15*, 190-196.

[63] El-Sherbiny, I. M.; Yacoub, M. H. "Hydrogel scaffolds for tissue engineering: Progress and challenges." *Global Cardiology Science & Practice* **2013**, *2013*, 316-342.

[64] Zhu, J.; Marchant, R. E. "Design properties of hydrogel tissue-engineering scaffolds." *Expert review of medical devices* **2011**, *8*, 607-626.

[65] Lakhtakia, A.; Martín-Palma, R. J. *Engineered Biomimicry*; Elsevier Science, 2013.

[66] Caliari, S. R.; Burdick, J. A. "A practical guide to hydrogels for cell culture." *Nat Meth* **2016**, *13*, 405-414.

[67] Campbell, P. K.; Bennett, S. L.; Driscoll, A.; Sawhney, A. S. ŧEvaluation of Absorbable Surgical Sealants : In Vitro Testing ŧ Covidien Laboratories, 2007.

[68] Peak, C. W.; Wilker, J. J.; Schmidt, G. "A review on tough and sticky hydrogels." *Colloid and Polymer Science* **2013**, *291*, 2031-2047.

[69] Barrett, D. G.; Bushnell, G. G.; Messersmith, P. B. "Mechanically Robust, Negative-Swelling, Mussel-Inspired Tissue Adhesives." *Advanced Healthcare Materials* **2013**, *2*, 745-755.

[70] Phadke, A.; Zhang, C.; Arman, B.; Hsu, C.-C.; Mashelkar, R. A.; Lele, A. K.; Tauber, M. J.; Arya, G.; Varghese, S. "Rapid self-healing hydrogels." *Proceedings of the National Academy of Sciences* **2012**, *109*, 4383-4388.

[71] Bait, N.; Grassl, B.; Derail, C.; Benaboura, A. "Hydrogel nanocomposites as pressure-sensitive adhesives for skin-contact applications." *Soft Matter* **2011**, *7*, 2025-2032.

[72] Algi, M. P.; Okay, O. "Highly stretchable self-healing poly(N,N-dimethylacrylamide) hydrogels." *European Polymer Journal* **2014**, *59*, 113-121.

[73] Yang, W. J.; Tao, X.; Zhao, T.; Weng, L.; Kang, E.-T.; Wang, L. "Antifouling and antibacterial hydrogel coatings with self-healing properties based on a dynamic disulfide exchange reaction." *Polymer Chemistry* **2015**, *6*, 7027-7035.

[74] Taylor, D. L.; in het Panhuis, M. "Self-Healing Hydrogels." *Advanced Materials* **2016**, *28*, 9060-9093.

[75] Asoh, T.-A.; Kikuchi, A. "Electrophoretic adhesion of stimuli-responsive hydrogels." *Chemical Communications* **2010**, *46*, 7793-7795.

[76] Asoh, T.-A.; Kawamura, E.; Kikuchi, A. "Stabilization of electrophoretically adhered gel-interfaces to construct multi-layered hydrogels." *RSC Advances* **2013**, *3*, 7947-7952.

[77] Asoh, T.-A.; Kikuchi, A. "Rapid fabrication of reconstructible hydrogels by electrophoretic microbead adhesion." *Chemical Communications* **2012**, *48*, 10019-10021.

[78] Asoh, T.-A.; Kinoshita, H.; Shoji, T.; Kikuchi, A.; Tsuboi, Y. "Rapid hydrogel repair utilizing microgel architectures." *Materials Chemistry Frontiers* **2017**, *1*, 1594-1599.

[79] Cayre, O. J.; Chang, S. T.; Velev, O. D. "Polyelectrolyte Diode: Nonlinear Current Response of a Junction between Aqueous Ionic Gels." *Journal of the American Chemical Society* **2007**, *129*, 10801-10806.

[80] Antipov, A. A.; Sukhorukov, G. B.; Donath, E.; Möhwald, H. "Sustained Release Properties of Polyelectrolyte Multilayer Capsules." *The Journal of Physical Chemistry B* **2001**, *105*, 2281-2284.

[81] Kato, M.; Tsuboi, Y.; Kikuchi, A.; Asoh, T. A. "Hydrogel Adhesion with Wrinkle Formation by Spatial Control of Polymer Networks." *J Phys Chem B* **2016**, *120*, 5042-6.

[82] Hosta-Rigau, L.; Chung, S. F.; Postma, A.; Chandrawati, R.; Städler, B.; Caruso, F. "Capsosomes with “Free-Floating” Liposomal Subcompartments." *Advanced Materials* **2011**, *23*, 4082-4087.

[83] van Dongen, S. F. M.; Nallani, M.; Cornelissen, J. J. L. M.; Nolte, R. J. M.; van Hest, J. C. M. "A Three-Enzyme Cascade Reaction through Positional Assembly of Enzymes in a Polymersome Nanoreactor." *Chemistry – A European Journal* **2009**, *15*, 1107-1114.

[84] Hosta-Rigau, L.; Shimoni, O.; Städler, B.; Caruso, F. "Advanced Subcompartmentalized Microreactors: Polymer Hydrogel Carriers Encapsulating Polymer Capsules and Liposomes." *Small* **2013**, *9*, 3573-3583.

[85] De Geest, B. G.; De Koker, S.; Immesoete, K.; Demeester, J.; De Smedt, S. C.; Hennink, W. E. "Self-Exploding Beads Releasing Microcarriers." *Advanced Materials* **2008**, *20*, 3687-3691.

[86] Pekarek, K. J.; Jacob, J. S.; Mathiowitz, E. "Double-walled polymer microspheres for controlled drug release." *Nature* **1994**, *367*, 258-60.

[87] Chang, T. M. S.; MacIntosh, F. C.; Mason, S. G. "SEMIPERMEABLE AQUEOUS MICROCAPSULES: I. PREPARATION AND PROPERTIES." *Canadian Journal of Physiology and Pharmacology* **1966**, *44*, 115-128.

[88] Chang, T. M. S. "Therapeutic applications of polymeric artificial cells." *Nat Rev Drug Discov* **2005**, *4*, 221-235.

[89] Salánki, R.; Hős, C.; Orgovan, N.; Péter, B.; Sándor, N.; Bajtay, Z.; Erdei, A.; Horvath, R.; Szabó, B. "Single Cell Adhesion Assay Using Computer Controlled Micropipette." *PLOS ONE* **2014**, *9*, e111450.

[90] "Micromanipulation." *can be accessed at* https://www.nikoninstruments.com/Learn-Explore/Techniques/Micromanipulation.

[91] Yoon, E.-S.; Singh, R. A.; Oh, H.-J.; Kong, H. "The effect of contact area on nano/micro-scale friction." *Wear* **2005**, *259*, 1424-1431.

[92] Davis, C. S.; Martina, D.; Creton, C.; Lindner, A.; Crosby, A. J. "Enhanced Adhesion of Elastic Materials to Small-Scale Wrinkles." *Langmuir* **2012**, *28*, 14899-14908.

List of Publications

1. A. Lu, Y. Liu, H. Oh, **A. Gargava**, E. Kendall, Z. Nie, D. DeVoe, S. R. Raghavan, "Catalytic Propulsion and Magnetic Steering of Soft, Patchy Microcapsules: Ability to Pick-Up and Drop-Off Microscale Cargo", *ACS Applied Materials & Interfaces,* **2016,** 8 (24), 15676-15683.

2. **A. Gargava**, C. Arya, S. R. Raghavan, "Smart Hydrogel-Based Valves Inspired by the Stomata in Plants", *ACS Applied Materials & Interfaces,* **2016,** 8 (28), 18430-18438.

3. J. Athas, C. Nguyen, B. Zarket, **A. Gargava**, Z. Nie, S. R. Raghavan, "Enzyme-Triggered Folding of Hydrogels: Towards a Mimic of the Venus Fly Trap", *ACS Applied Materials & Interfaces,* **2016,** 8 (29), 19066-19074.

4. T. Guo, T. Holzberg, C. Lim, F. Gao, **A. Gargava,** J. Trachtenberg, A. Mikos, J. Fisher, "3D Printing PLGA: A Quantitative Examination of the Effects of Printing Parameters on Print Resolution", *Biofabrication,* **2017,** 9 (2), 024101.

5. **A. Gargava**, S. R. Raghavan, "Electro-Formation of Alginate Gels", in preparation.

6. **A. Gargava**, S. R. Raghavan, "Electrically Induced Rupture of Microparticles", in preparation.

7. **A. Gargava**, S. R. Raghavan, "Electrically Induced Adhesion of Beads to Gels", in preparation.

List of Conference Presentations

1. **A. Gargava**, R. Ragunathan, S. R. Raghavan, "Shape changes in hybrid hydrogels: Mimicking biological processes in plants", *88th ACS Colloid and Surface Symposium*, **2014**, Philadelphia, Pennsylvania.

2. **A. Gargava**, R. Ponte, R. Ragunathan, S. R. Raghavan, "Electrically induced controlled release from biopolymer capsules", *89th ACS Colloid and Surface Symposium*, **2015**, Pittsburgh, Pennsylvania.

3. **A. Gargava**, R. Ponte, R. Ragunathan, S. R. Raghavan, "Electrically induced controlled release from biopolymer capsules", *AICHE Annual Meeting,* **2015**, Salt Lake City, Utah.

4. **A. Gargava**, J. C. Athas, S. R. Raghavan, "Rapid electro-formation of robust and transparent biopolymer gels in prescribed 3-D shapes", *89th ACS Colloid and Surface Symposium*, **2016**, Cambridge, Massachusetts.

5. **A. Gargava**, S. R. Raghavan, "Electrically induced controlled release from biopolymer capsules", *253rd American Chemical Society National Meeting and Exposition,* **2017**, San Francisco, California.

6. **A. Gargava**, S. R. Raghavan, "Smart hydrogel-based valves inspired by the stomata in plants: Ability to regulate water flow based on temperature, pH, and light", *253rd American Chemical Society National Meeting and Exposition,* **2017**, San Francisco, California.

7. **A. Gargava**, S. R. Raghavan, "Rapid electro-formation of robust and transparent biopolymer gels in prescribed 3-D shapes", *2017 MRS Spring Meeting and Exhibit*, **2017**, Phoenix, Arizona.